A THESIS

FOR THE DEGREE OF MASTER OF SCIENCE

Protective effect of a freshwater algae *Spirogyra* sp. against skin aging induced by ultraviolet-B irradiation

Lei Wang

Department of Marine Life Science

GRADUATE SCHOOL

JEJU NATIONAL UNIVERSITY

February, 2016

Protective effect of a freshwater algae *Spirogyra* sp. aginst skin aging induced by ultraviolet-B irradiation

Lei Wang

(Supervised by Professor You-Jin Jeon)

A thesis submitted in partial fulfillment of the reqiurement for the degree of Master of Science

February, 2016

This thesis has been examined and approved by

Thesis director, Seon Heui Cha, Ph.D, School of Medicine, Ajou University

Joon Bum Jeong, Professor of Marine Life Science

School of Marine Biomedical Science, Jeju National University

You-Jin Jeon, Professor of Marine Life Science

School of Marine Biomedical Science, Jeju National University

02/2016

Data

Department of Marine Life Science

GRADUATE SCHOOL

JEJU NATIONAL UNIVERSITY

CONTENTS

Abstract

Spirogyra sp. a freshwater algae, was collected during Januray to March in Kongju, South Korea. The lyophilized sample was extracted by 70% ethanol and obtained the 70% ethanol crude extract (SPE). The free radical scavenging activities and protective effects against skin aging induced by UV-B irradiation of SPE were evaluated in vitro on HaCaT cell line. The results suggests that SPE have protective effects against skin aging. Then, SPE was fractionated by organic solvets based on polarity. The ethyl actate fraction (SPEE) was found to contain a higher phenolic content than the other fractions, so it was selected for futher studies. The protective effects of SPEE against skin aging induced by UV-B irradiation were evaluated in vitro on HaCaT cell line and in vivo on zebrafish model. Anti-aging compounds of SPEE were seperated by one step using preparative centrifugal partition chromatography (CPC). This study suggests that *Spirogyra* sp. was rich in phenolic content and have strong radical scavenging activities and anti-UV-B irradiation activity. It has the potential to be used as a promising ingredient in cosmetic industry.

List of figures

min: 25:75 v/v ; 30-80 min: 50:50 v/v ; 80-90 min: 100:0 v/v; 90-110 min: 100:0 v/v); flow rate 0.3 mL/min ; detected wave length was 220 nm. ABTS solution eluted at flow rate 1.0 mL/min and measured as negative peak by UV/Vis detector at a wave length of 680 nm.

Fig. 8. Cell viability of HaCaT cells after treated SPE. HaCaT cells were seeded in 96-well plate at a concentration of 1.0×10^5 cells/mL. Cell viability was determined by MTT assay. Experiments were performed in triplicate and the data are expressed as mean ± SE.

Fig. 9. Intracellular ROS scavenging activity of SPE in HaCaT cells, HaCaT cells were seeded into a 24-well plate at a concentration of 2.0×10^5 cells/mL. Cellular ROS level were determined by DCF-DA analysis. Experiments were performed in triplicates and the data are expressed as mean ± SE. * $p<0.05$.

Fig. 10. Cytoprotective effect of SPE in HaCaT cells. HaCaT cells were seeded into a 24-well plate at a concentration of 2.0×10^5 cells/mL. Cell damage degree and viability were determined by LDH and MTT analysis. (A): LDH release level**,** (B): cell viability. Experiments were performed in triplicate and the data are expressed as mean ± SE. * $p<0.05$. ** $p<0.001$.

Fig. 11. The procedure of fractionation of SPE using different solvents. After fractionation, the 4 fractions were collected and named as SPEH, SPEC, SPEE and SPEW respectively.

Fig. 12. DPPH radical scavenging activity of SPEE. DPPH radical scavenging activity was determined by ESR. Experiments were performed in triplicate and the data are expressed as mean ± SE.

Fig. 13. Alkyl radical scavenging activity of SPEE. Alkyl radical scavenging activity was determined by ESR. Experiments were performed in triplicate and the data are expressed as mean ± SE.

Fig. 14. Hydroxyl radical scavenging activity of SPEE. Hydroxyl radical scavenging activity was determined by ESR. Experiments were performed in triplicate and the data are expressed as mean ± SE.

Fig. 15. Hydrogen peroxide scavenging activity of SPEE. Hydrogen peroxide scavenging activity was determined by colorimetic method. Experiments were performed in triplicate and the data are expressed as mean ± SE.

Fig. 16. On-line HPLC analysis of SPEE. (A) HPLC chromatogram, (B) $ABTS^{+}$ absorption sepectrum. Colunm: SunFire 5μm ODS column (4.6 × 250 mm i.d.); mobile phase: acetonitrile-distilled water solvent system(0-10 min: 20:80 v/v; 10-30 min: 25:75 v/v ; 30-50 min: 27:73 v/v ; 50-60 min: 30:70 v/v; 60-70 min:50:50 v/v; 70-80 min:100:0 v/v); flow rate 1.0 mL/min; detected wave length was 290 nm. ABTS solution eluted at flow rate 1.0 mL/min and measured as negative peak by UV/Vis detector at a wave length of 680 nm.

Fig. 17. Cytotoxicity analysis of SPEE. HaCaT cells were seeded in 96-well plate at a concentration of 1.0×10^5 cells/mL. Cell viability was determined by MTT assay. Experiments were performed in triplicate and the data are expressed as mean ± SE.

Fig. 18. Intracellular ROS sacvenging activity of SPEE in HaCaT cells. HaCaT cells were seeded in a 24-well plate at a concentration of 2.0×10^5 cells/mL. Cellular ROS level was determined by DCF-DA analysis. Experiments were performed in triplicate and the data are expressed as mean ± SE. * $p<0.05$.

Fig. 19. Cytoprotective effect of SPEE in HaCaT cells. HaCaT cells were seeded in a 24-well plate at a concentration of 2.0×10^5 cells/mL. Cell damage degree and viability were determined by LDH and MTT analysis. (A): LDH release level**,** (B): cell viability. Experiments were performed in triplicate and the data are expressed as mean ± SE. * $p<0.05$.

Fig. 20. Apototic body formation under UV-B irradiation. HaCaT cells were seeded in a 24-well plate at a concentration of 2.0×10^5 cells/mL. After 24 h incubation cells were pretreated with sample. After 2 h incubation, cells were exposed to 30 mJ/cm^2 UV-B and incubated 6 h. After incubation, cells were stained with Hoechest 33342, then, the nuclear morphology of cells were examined by microscope.

Fig. 21. Cell cycle analysis. HaCaT cells were seeded in a 24-well plate at a concentration of 2.0×10^5 cells/mL. After 24 h incubation cells were pretreated with sample. After 2 h incubation, cell were exposed to 30 mJ/cm^2 UV-B and incubated 6 h. After incubation, cells were collected and fixed by 70 % ethanol, Then the cells were incubated in dark with 1 mL EDTA which contained 100 μg PI and 100 μg Rnase A for 30 min at 37 ℃. Cell cycle analysis was conducted with FACS calibur flow cytometer.

Fig. 22. ROS generation in SPEE pre-treated zebrafish. The 2 dpf zebrafish embryos were used for the anti-UV-B study. At 2 dpf, the embryos were treated with sample. After 1 hour, the embryos were exposed to 50 mJ/cm^2 UV-B per individual. After irradiating embryos with UV-B, the embryos were treated with DCFH-DA solution (20 μg/mL) and incubated for 1 hour in the dark at 28.5℃. After anesthetized, the embyros were photographed under the microscope. The individual zebrafish larvae fluorescence intensity was quantified using an image J program. (A): The phptograph

under fluorescence microscop, (B): The level of ROS generation in zebrafish. Experiments were performed in triplicates and data were expressed as mean ± SE. * $p<0.05$.

Fig. 23. The HPLC chromatogram of SPEE. Colunm: SunFire 5μm ODS column (4.6 × 250 mm i.d.); mobile phase: acetonitrile-distilled water solvent system(0-10 min: 20:80 v/v; 10-30 min: 25:75 v/v ; 30-50 min: 27:73 v/v ; 50-60 min: 30:70 v/v; 60-70 min:50:50 v/v; 70-80 min:100:0 v/v); flow rate 1.0 mL/min; detected wave length was 290 nm.

Fig. 24. The CPC chromatogram of SPEE. Solvent condition: stationary phase, bottom aqueous; mobile phase, top organic phase; rotation speed: 1000 rpm; flow rate: 2 mL/min; sample: a weight of 500 mg of sample dissolved in 6 mL misture of top and bottom phases (1:1,v/v) of the solvent system; UV detector at a wave length of 254 nm; fractions from the CPC were collected in to text tubes using a fraction collector.

Fig. 25. Analysis of the fractions collected by CPC using HPLC (A) SPEE, (B) traget-1,(C) traget-2, (D) traget-3, (E) traget-4, (F) traget-5, (G) traget-6, (H) traget-7.

Fig. 26. The chemical structure of gallic acid and methyl gallate. (A) Gallic acid, (B) methyl gallate.

Fig. 27. DPPH radical scavenging activity of SPE. DPPH radical scavenging activity was determined by ESR. Experiments were performed in triplicates and data are expressed as mean ± SE.

List of tables

1. Introduction

Microalgae are a group of algae that grows in freshwater and marine eco-systems. They are also being cultured in freshwater or seawater conditions mainly for the purpose of industrial or academic research. Microalgae are unicellular organisms that can exist individually, or in chains or groups. Microalgae have been found to produce a variety of primary and secondary metabolites similer to that of plants. Because they produce a variety of secondary metabolites, they are being utilized in many kinds of areas such as biodiesel production, phamaceutical applications and functional food applications. Extensive research have been carried out about biodiesel production using microalgae during the past few decades (Li Y et al., 2008, Li Y et al, 2008, Sheehan J et al., 1998). This has become an interesting area of research due to the higher consumption and reduction of natural oil resource worldwide. Secondary metabolites synthesized by microalgea that includes sterols, fatty acids, polyphenols and terpenoids have been found to indicate antioxidant, anticancer, antiflammatory and a range of other bioactivities (VALERIE J. PAUL et al., 1986, Zhongshan Zhang et al., 2010). According to Mayalen Zubia, phenolic content and antioxidant activities of 48 species of marine microalgae were evaluated. Some research suggest that some microalgae which were rich in phenolic composition have a good antioxidant activities (Mayalen Zubia et al., 2007). Many studies have focused on the use of microalgae as functional food material and according to several reports many microalgae had been used as ingredients in food items (Merichel Plaza et al., 2008). Due to the fact that microalgae indicates potential biological functionalities they are attaining an increased interest in a various type of research areas as potential candidates for pharmaceutical, functional food and other industrial applications.

Spirogyra sp. is a freshwater green alga that commonly inhabit freshwater areas such as shallow ponds. There are more than 400 species of *Spirogyra* organisms, such as *Spirogyra charophyta*, *Spirogyra zygenmaceae*, *Spirogyra acumbentis* and other species. Morphologically, *Spirogyra* sp. are filamentous and exists in shallow ponds. Because of the special structure characteristic of *Spirogyra* sp., they were used as a biosorbent to remove heavy metal ions from wastewaters. Many research demonstrates that *Spirogyra* sp. is capable of absorbing and accumulating heavy metals like plumbum, chromium, copper, zinc and fluorides (V.K. Gupta et al., 2006, V.K. Gupta et al., 2006, V.K. Gupta et al., 2001, N.R. Bishnoi et al., 2005, S. Venkatamohan et al., 2007). Many research reports the use of *Spirogyra* sp. as a material in producing bioenergy. Fuad Salem Eshaq et al. cultured and used *Spirogyra* sp. as a material for the production of biofuel (Fuad Salem Eshaq et al., 2010). According to Rameshprabu Ramaraj et al., *Spirogyra ellipsospora* was cultured and used for the production of biogas by anaerobic fermentation (Rameshprabu Ramaraj et al., 2015). The chemical composition of *Spirogyra* sp. indicates a great diversity such as sterols, pigments, carbohydrates, monosaccharides, polysaccharides, and other compounds (Maya Iv. Mitova et al.,1999). Several of these compounds have been used in medical and functional food areas. Ji-Hyeok Lee et al. isolated two phenolic compounds that includes gallic acid and methyl gallate from *Spirogyra* sp. and evaluated the protective effects of *Spirogyra sp.* against lipid peroxidation (Ji-Hyeok Lee et al., 2015). Nalea Kang et al. investigated the effects of *Spirogyra* sp. to improve cardiovascular diseases (Nalae Kang, et al., 2015). Several research suggest the use of *Spirogyra sp.* as a potential ingredient in biomedical research that can be used in pharmaceutical and functional food applications.

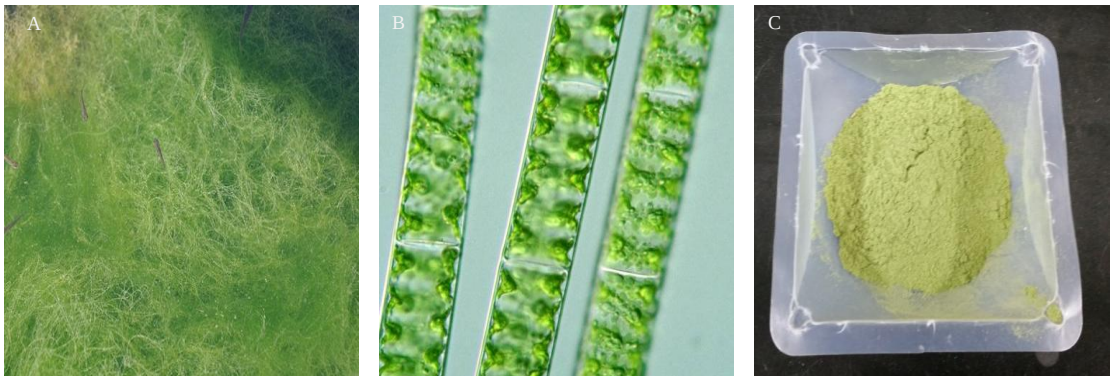

Fig. 1. The photograph of *Spirogyra* sp.. A. *Spirogyra* sp. in the shallow pond.

B. *Spirogyra* sp. at microscope. C. The lyophilized powder of *Spirogyra* sp.

Oxidative stress, is a state in which there is an imbalance between cellular pro-oxidant and antioxidant levels. In aerobic organisms, reactive oxygen species (ROS) are the most abundant pro-oxidant generated due to the body respiration and metabolism (E.Herrero et al., 2008, Kasidit Rattanawong et al., 2015). ROS, such as superoxide anion radical (O^{2-}), hydrogen peroxide peroxide (H_2O_2), hydroxyl radical (OH^-) and singlet oxygen ($^1O_2$), plays an important role in oxidative stress (S.S. Gill et al., 2010). The effects of ROS can be thought of as a double-edged sword, whereas on the one hand it reduces the amount of intracellular ROS that regulate cellular functions, and as on the other hand, it induces oxidative stress (Guan-qun Chen et al., 2015). Normally, it is a dynamic balance between ROS generation and degradation in the normal physiological condition of human bodies because of the endogenic antioxidant system of cells. But in some pathological conditions, this balance will be broken. Cells generated and accumulated with many ROS are central to oxidative stress-related metabolism (Guan-qun Chen et al., 2015). Overproduction of ROS induces oxidative stress. Because of ROS damage many cellular composition and cellular structures, including DNA, proteins, lipids and cell membranes. Thus, ROS have been found to induce a large number of disease conditions such as cancer, inflammation, aging and some metabolic syndromes (Hyemin Kim et al., 2013, Mingjing Gao et al., 2015, Nassima Chaher et al., 2016). Because of the imbalance of ROS generation and degration that brings harmful effects on human bodies, more researchers are interested in funding ROS scavengers as exogenous antioxidants to scavenge spare ROS generated in cells due to some pathological conditions.

Ultraviolet (UV), is a natural component of sunlight. It is an electromagnetic radiation spanning within the wavelength region from 400 nm to 100 nm. Normally, it is invisible and can be separate to 3 subtypes based on the wavelength. The wavelength region from 320 to 400 nm can be called UV-A, the wavelength region from 280 to 320 nm is UV-B and wavelength region from 100 to 280 nm is UV-C (Song-Zhi Kong et al., 2015). From this three subtypes, UV-B is the one which attract more attention that brings stress to plants and animals including human (Moirangthem Kameshwor Singh et al., 2015). Of this three subtypes of UV, UV-B is the one that have a medium wavelength which plays an important role in skin aging and some skin diseases. UV-B irradiation can directly damage the epidermis of skin by inducing cellular ROS generation and damage cellular compositions and structures such as protein, lipid, DNA. Normally, most of UV-B coming from sunlight can be abosorbed by the ozone layer. But, the ozone layer is becoming thinner due to anthropogenic activities. Nowadays, the UV-B irradiation intensities in the biosphere has increased compared with previous times (Meiling Liu, et al., 2015). With increased amounts of UV-B irradiation in biosphere, there is increased issues. For humans, it already become one of a serious threat for their health.

Human, skin is one of the most important organ in the body because of its important protective functions. Skin plays a protective function in the human bodies. Aging is a serious and prominent problem of skin (Sushil Raut et al., 2012). The factors which induced skin aging can be distinguished as two types based on the characteristics of those factors as intrinsic and extrinsic factors (Farage et al., 2008, A. Kammeyer and R.M.Luiten, 2015). All of those factors are leading to reduce the structural integrity of skin because of the increasing ROS generation, thus loss of physiological functions (Landau, 2007). Skin aging is mainly induced by ROS, as these ROS are involved in

stimulating intracellular and extracellular oxidative stress (Masaki, H. ,2010). Intrinsic oxidative stress is a natural aging process that brings degenerative effects to the human body induced by the genetic factors and hormonal changes. Extrinsic oxidative stress is induced by many enviromental factors such as smoking, UV exposure, air pollutants, illnesses, lack of nutrition and other factors (Farage et al., 2008; Pinnell, 2003). UV-exposure and smoking are two typical extrinsic factors for skin aging. Especially for the individuals who are not engaged in smoking, UV-exposure is a harmful extrinsic factor that induce skin aging.

2. Meterials and methods

2.1. Chemicals and reagents

The fluorescent probe 2', 7'-dichlorodihydroflurescin diacetate (DCFH-DA) and 3-(4-5- dimethyl-2yl)-2-5-diphynyltetrasolium bromide (MTT), Dimethyl sulfoxide (DMSO) and phosphate buffered saline (PBS), standard gallic acid, Neohesperidin1, 1-diphenyl-2-picrylhydrazyl (DPPH), 2,2-azobis (2-amidinopropane) hydrochloride (AAPH), 5,5-dimethyl-1-pyrolin N-oxide (DMPO), 2,2'-azino-bis(3-ethylbenzothiazoline-6-sulphonic acid (ABTS) and α-(4-Pyridyl-1-oxcide)-N-ter-butylnitrone (POBN) were purchased from Sigma Co. (St. Louis, MO, USA). HPLC-grade acetonitrile was purchased from Burdick & Jackson (USA). The Dulbecco's modified Eagle medium (DMEM), Penicillin / streptomycin and fetal bovine serum (FBS) were purchased from Sigma Co. (St. Louis, MO, USA). $FeSO_4 \cdot 7H_2O$ and H_2O_2 and the sovents used for CPC were purchased from Fluka Co. (Buchs, Switzerland). All other chemicals used in this study were of analytical grade.

2.2. Sample collection and pre-processing

Spirogyra sp. sample was collected in spring season, in January 2014, in shallow ponds of Kongju, South Korea (36°20′34″, 127°12′ 28″). The algae were washed with fresh water to remove other impurities. After washing, the algae were freeze-dried and then ground, and sifted through a 50-mesh standard testing sieve. The dried algae powder were stored at -20℃ in refrigerator until use.

2.3. Extraction of 70% crude ethanol extract

Lyophilized algae powder with a weight of 10 g was mixed with 1 L 70 % ethanol under continuous shaking at 120 rpm for 24 hours at 25℃ without light and filtered though Whatman No:4 filter paper. The above procedure was repeated until the extract is colorless. All the extracts were combined, and the extracts were concentrated by rotary evaporator at a low pressure. Finaly obtained the 70 % ethanol crude extract of *Spirogyra* sp. which will be reffered to as SPE.

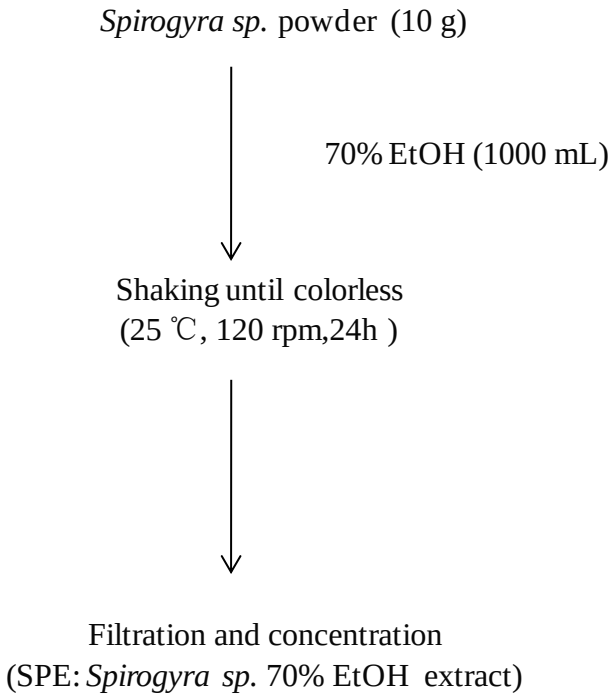

Fig. 2. The extraction procedure. Lyophilized algae was extracted with 70% EtOH, and concentrated by using rotary evaporator at a low pressure. The crude extract named as SPE.

2.4. Sample preparation

Sampes were dissolved in dimethy sulfoxide (DMSO) to prepare a 100 mg/mL stock solutions. Stock solutions were diluted with distilled water (D.W) to get the serious of concentractions which were used during the study. For cell experiments, samples were diluted with 1X phosphate buffer (PBS) from stock solution and filtered using a 0.45 μm syringe filter.

2.5. Determination of total phenolic content of samples

The total phenolic content of the samples were deterimined based on the method described by Chandler and Dodds with slight modifications (Chandler, S.F.,1983; Mahinda Senevirathne et al, 2015). Beiefly, one milliliter of 0.1 mg/mL of sample solutions were mixed in a test tube containing 1 mL of 95% ethanol, 5 mL of distilled water. Then, 0.5 mL of 50% Folin–Ciocalteu reagent was added to the test tubes sequentially and mixed thoroughly using the vortex mixer. The mixture was allowed to reaction for 5 minutes in the dark, and 1 mL of 5% Na_2CO_3 solution was added to each test tube, after it was mixed thoroughly using a vortex mixer, it was kept in dark for 1 hour. The absorbance was recorded at 700 nm using an enzyme-linked immunosorbent assay (ELISA) microplate reader (Sunrise,Tecan Co.Ltd., Australia). Gallic acid was used as the reference phenolic compound to construct the standard curve to calculation the phenolic content of samples.

2.6. Determination of DPPH radical scavenging activity of samples

The DPPH radical scavenging activity of the samples were determined by Electron Spin Resonance (ESR) spectrometry (JES-FA machine, JOEL, Tokyo, Japan). The experimental method was adupted from the method described by Nanjo et al with slight modifications (Nanjo, F., Goto, K. 1996). Briefly, DPPH was dissolved in methanol at a concentration 60 μmol/L. A 40 μL of freshly prepared DPPH was added to the same volume of samples with different concentrations separately. After 10 seconds of vortexing, the solutions were kept at room temprature for 2 min for the reaction. After incubation, the solutions were transferred to a 50 μL glass capillary tube and fitted into the cavity of the ESR spectrometer. The measurements were taken under following conditions, central field 3475 G; modulation frequency 100 kHz; modulation width 0.8 mT; amplitude 1000 mT; sweep width 10 mT; microwave power 1 mW and temperature 298 K.

2.7. Determination of alkyl radical scavenging activity of samples

The alkyl radicals were generated by 2,2-azobis (2-amidinopropane) hydrochloride (AAPH). The reaction mixture was composed of 20 μL of distilled water, 20 μL of sample solutions with a different concentration, 20 μL of 40 mM AAPH and 20 μL of 40 mM POBN. The solutions were mixed by vortexing and incubated at 37 ℃ in a water bath for 30 min. After that, the reactants were transferred into 50 μL glass capillary tubes and placed in the ESR spectrometer. The measurement conditions were as follows: central field 3475 G, modulation frequency 100 kHz, modulation width 0.2 mT, amplitude 1000 mT, sweep width 10 mT, microwave power 1 mW and temperature 298 K.

2.8. Determination of hydroxyl radical scavenging activity of samples

Hydroxyl dadicals were generated by the Fenton reaction ($Fe^{2+}+H_2O_2 \rightarrow HO^{\cdot}+OH^{-}$), and reacted rapidly with nitrone spin trap DMPO, the product DMPO-OH adducts is detectable with ESR spectrometer. The reaction system was composed of 20 μL of sample, 20 μL of 0.3 M DMPO, 20 μL of 10mM $FeSO_4$ $7H_2O$ and 20 μL of 10 mM H_2O_2. After mixing the contents thoroughly by vortex, the reactants were allowed react for 2.5 min at room temperature. Then the ESR spectrum of the remaining DMPO-OH adducts of each sample mixture was recorded using the following ESR conditions, central field 3475 G, modulation frequency 100 kHz, modulation width 0.1 mT, amplitude 200 mT, sweep width 10 mT, microwave power 1 mW and temperature 298 K.

2.9. Determination of hydrogen peroxide scavenging activity of samples

The hydrogen peroxide scavenging activity of samples were determined by colorimetric methods. The reaction mixture containing 50 μL of 0.1 M phosphate buffer (PH = 5), 50 μL sample solutions was mixed with different concentrations and 10 μL of 10 mM hydrogen peroxide peroxide. After filled above solution in 96-well plate, the plate was incubate at 37 ℃ for 5 min. After incubation, 15 μL of 1.25 mM ABTS and 15 μL of peroxidase were added into the plate, and incubate at 37 ℃ for 10 min. After incubation, the absorbance was recorded at 405 nm using an ELISA microplate reader (Sunrise,Tecan Co.Ltd., Australia).

2.10. Determination of ABTS radical scavenging activity of SPE by on-line High Performance Liquid Chromatography (HPLC) system

The ABTS radical scavenging activity of SPE was analysed by on-line HPLC system. 2 mM ABTS radical solvent that containing 2.5 mM potassium persulfate was prepared and incubated for 24 hours to stabilized the radical befor using. HPLC system equipted with binary Waters 515 pump, Waters 2489 UV/Vis and 2998 photodiode array (PDA) detector and Waters 2707 autosampler. HPLC system is coupled with the interface $ABTS^{+}$ radical analyzer (Waters, Mailford, MA 01757, USA). SPE was dissolved in methanol as a concentration of 5 mg/mL. 10 μL of sample was injected to a Atalantis T3 3 μm 3.0 × 150 mm column (Waters, USA) and run at 0.3 mL/min flow rate using a gradient of Acetonitrile (ACN) and distilled water (D.W) solvent system, 0-10 min: 0 % ACN and 100 % D.W, 10-30 min 25 % ACN and 75 % D.W, 30-80 min 50 % ACN and 50 % D.W, 80-90 min 100 % ACN and 0 % D.W, 90-110 min 100 % ACN and 0 % D.W and detected wave length was 220 nm. The sample was eluted though the column, the elution was go to react with ABTS radical in the reaction coil at 40℃. Absorbance of the reaction mixture was measured as negative peak by UV/Vis detector at a wave length of 680 nm.

2.11. Cell culture

Human Keratinocytes (HaCaT) cell line was purchased from Korean Cell Line Bank. The HaCaT cells were maintained in DMEM supplemented with 10% heat-inactivated FBS, streptomycin (100 μg/mL), penicillin (100 unit mL^{-1}) at 37℃ in an incubator under humidified atmosphere containing 5% CO_2.

2.12. Determination of cytotoxicity of samples in HaCaT cells

The cytotoxicity of samples were evaluated by MTT assay described by Mosmann Rosen, G.M., Rauckman (Rosen,G.M., Rauckman, 1980). The HaCaT cells were seeded in 96-well plate at a concentration of 1.0×10^5 cells/mL. After 24 h of incubation at 37℃, the cells were treated with 10 μL of samples which carried a final concentration of 6.25, 12.5, 25, 50, 100 and 200 μg/mL and the control groups were treated with same volume of 1X PBS. After sample treatment, the cells were incubated for 24 h at 37℃. Then, a volume of 50 μL of MTT stock solution (2 mg/mL) was applied to each well. After 3 h incubation, the supernatant was aspirated. The formazan crystals in each well were dissolved in 150 μL DMSO, and the absorbance was meassured by ELISA microplate reader at 540 nm wave length. The cell viability of control groups were be thought as 100 %.

2.13. Determination of intracellular ROS generation induced by UV-B irradiation in HaCaT cells

HaCaT cells were seeded in a 24-well plate at a concentration of 2.0×10^5 cells/mL and incubated at 37℃ for 24 h. After incubation, cells were treated with sample solutions that carries a final concentration of 12.5, 25, 50 and 100 μg/mL and incubated for 30 min at 37℃. Then, the cells were treated with DCFH-DA (500 μg/mL) and incubated 30 min at 37℃. After incubation, medium was removed, and cells were washed with 1X PBS two times. After washing, cells were repleced with 200 mL fresh 1X PBS and exposed to 30 mJ/cm^2 of UV-B light using a UV-B meter (UV Lamp, VL-6LM, Vilber Lourmat, France) and the fluorescence emission of DCF-DA was detected at an excitation wavelength of 485 nm and emission wavelength of 535 nm, using a spectrofluorometer.

2.14. Determination of cytoprotective effect of samples against UV-B irradiation in HaCaT cells

HaCaT cells were seeded in a 24-well plate at a concentration of 2.0×10^5 cells/mL and incubation at 37 ℃ for 24 h. After incubation, cells were treated with sample solutions that carries a final concentration of 12.5, 25, 50 and 100 μg/mL and incubated for 2 hours at 37 ℃. After incubation, the medium was removed, and cells were washed with 1X PBS two times. After washing, cell were repleced with 200 mL fresh 1X PBS and exposure to 30 mJ/cm^2 of UV-B light using a UV-B meter (UV Lamp, VL-6LM, Vilber Lourmat, France). Then, the PBS was removed and serum free DMEM medium was filled into each well and incubation for 24 hours. After incubation 24 hours, 50 μL supernatant of each well were transfred to a 96-well plate for LDH level analysis, and a volume of 100 μL of MTT stock solution (2 mg/mL)

was applied to each of each well. After 3 h incubation, the supernatant was aspirated and 400 μL DMSO was filled to each well to dissolved formazan crystals. The absorbance by ELISA microplate reader at wave length of 540 nm. The cell viability of control groups were be thought as 100 %.

2.15. Fractionation of SPE using different solvents

Dry SPE was fractionated by different polarity organic solvents that includes hexane, chloroform, ethyl acetate. The dry SPE sample, 1.9205 g was dissolved in distilled water and shaken with hexane for severals times until the hexane layer was colorless and combined all of hexane fractions together and concentrated by rotary evaporator at a low pressure. The remaining water layer continue shaken with chloroform for several times until the chloroform was colorless and combined all of chloroform fractions together and concentrated by rotary evaporator at a low pressure. And the remaining water layer fractionated by ethyl acetate and remaining water was considered as the water fraction. The hexane, chloroform, ethyl acetate and water fractions of SPE were named SPEH, SPEC, SPEE and SPEW respectively. All fractions were dried and keep in -20 ℃ refrigerator until used for further research.

2.16. Determination of ABTS radical scavenging activity of SPEE by on-line HPLC system

The ATBS radical scavenging activity of SPEE was evaluated by the $ABTS^{+}$ Online HPLC system. SPEE was dissolved in methanol as a concentration of 5 mg/mL. valume of 10 μL of sample was injected to a SunFire 5μm 4.6 × 250 mm column

(Waters, Ireland) and run at 1.0 mL/min flow rate using a gradient of ACN and D.W solvent system, 0-10 min: 20 % ACN and 80 % D.W, 10-30 min 25 % ACN and 75 % D.W, 30-50 min 27 % ACN and 73 % D.W, 50-60 min 30 % ACN and 70 % D.W, 60-70 min 50 % ACN and 50 % D.W, 70-80 min 100 % ACN and 0 % D.W and detected wave length was 290 nm. The sample was eluted though the column, the elution was go to reacted with ABTS radical in the reaction coil at 40 ℃. Absorbance of the reaction mixture was measured as negative peak by UV/Vis detector at a wave length of 680 nm.

2.17. Determination of apoptotic body formation by nuclear staining with Hoechest 33342.

HaCaT cells were seeded in a 24-well plate at a concentration of 2.0×10^5 cells/mL and incubated at 37℃ for 24 h. After incubation, cells were treated with SPEE solutions of final concentrations 25, 50 and 100 μg/mL and incubated for 2 hours at 37℃. After incubation, the medium was removed, and cells were washed with 1X PBS two times. After washing, cell were repleced with 200 mL fresh 1X PBS and exposure to 30 mJ/cm^2 of UV-B light using a UV-B meter. Then, the PBS was removed and serum free DMEM medium was filled into each well and incubated for 6 hours. Then, cells were treated with 25 μL of Hoechest 33342 (stock 10 mg/mL) and incubated for 10 min at 37℃. The stained cells were observed using a fluorescence microscope to examine apoptotic body formation.

2.18. Cell cycle analysis

HaCaT cells were seeded in a 6-well plate at a concentration of 4.0×10^5 cells/mL and incubated at 37 ℃ for 24 h. After incubation, cells were treated with SPEE solutions that carries a final concentrations of 25, 50 and 100 μg/mL and incubated for 2 hours at 37 ℃. After incubation, the medium was removed, and cells were washed with 1X PBS two times. After washing, cell were repleced with 200 mL fresh 1X PBS and exposedto 30 mJ/cm^2 of UV-B light using a UV-B meter. Then, the PBS was removed and serum free DMEM medium was filled into each well and incubated for 6 hours. The cells were harvested and washed two times with 1X PBS. After washing, cells were fixed in 1 mL 70 % ethanol for 30 min at 4℃. After cells were fixed by 70 % ethanol, cells were washed two times with 2 mM EDTA. Then the cells were incubated in dark with 1 mL EDTA containing 100 μg PI and 100 μg Rnase A for 30 min at 37℃. Cell cycle analysis was conducted with FACS calibur flow cytometer (Becton-Dickinson, San Jose ,CA,USA). The cell cycle phases were analysed by histograms given by the Quest and Mod-Fit computer programs (Sung-Myung Kang et al, 2012). The anti-apoptotic activity of SPEE on cell cycle was evaluated by change in the perentage of cell distribution at each cell cycle phase.

2.19. Origin and maintenance of parental zebrafish

The adult zebrafish were purchased from a commercial dealer (Seoul aquarium, Korea). And the fishe were separately kept in 3 Lacrylic tank in 28.5 ℃, with a 14/10 h light/dark cycle. Zebrafishes were fed 3 times/day, 6 days/week, with tetramin flake food supplemented with live brine shrimps. Embryos were obtained from natural

spawning that was induced in the morning by turning on the light. Collection of embryos were completed within 30 min.

2.20. Determination of UV-B protection effect of SPEE in vivo / in zebrafish mode

The ROS generation of zebrafish was analyzed using DCFH-DA that is an oxidantion sensitive flourescent probe dye. The 2 dpf embryos were used for the anti-UV-B study. At 2 dpf, the embryos were treated with SPEE solutions with a final concentration of 25, 50 and 100 μg/mL. After 1 hour, the embryos were washed with embryo media and exposed at 50 mJ/cm^2 UV-B individual. After irradiating embryos with UV-B, the embryos were transferred into 96-well plate and treated with DCFH-DA solution (20 μg/mL) and incubated for 1 hour in the dark at 28.5℃. Then , the embryos were washed two times with embryo media and anesthetized phenoxyethanol before visualization (Seok-Chun Ko et al, 2011). After anesthetized, the embyros were photographed under the microscope Cool SNAP-Procolor digital camera (Olympus, Japan). And the individual zebrafish larvae fluorescence intensity was quantified using an image J program.

2.21. Optimisation the Centrifugal Partition Chromatographic solvent system

The solvent system contained hexane, ethyl acetate, methanol and water with different ratio (H:EA:Me:W), the total valume of solvent system is 2 mL. Solvent of H:EA:Me:W were mixed with different ratio and kept some time until two phases reach the equilibrium. A volume of 500 μL of top phase and 500 μL of bottom phase

transferred into a micro tubes. Weight of 5 mg of SPEE was dissolved in the seperated solvent and mixed well. The micro tubes were centrifuged for 10 min and 200 μL of top phase and 200 μL of bottom phase were seperated in to different vials and dried by the rotary evaporator at a low pressure. The dry sample of each vials were dissolved in 500 μL methanol and analysed by HPLC. Volume of 10 μL of sample was injected to a SunFire 5 μm 4.6 × 250 mm column (Waters, Ireland) and run at 1.0 mL/min flow rate using a gradient of ACN and D.W solvent system, 0-10 min: 20 % ACN and 80 % D.W, 10-30 min 25 % ACN and 75 % D.W, 30-50 min 27 % ACN and 73 % D.W, 50-60 min 30 % ACN and 70 % D.W, 60-70 min 50 % ACN and 50 % D.W, 70-80 min 100 % ACN and 0 % D.W and detected wave length was 290 nm. The area under the curve was calculated for each separete peak. The distribution coeffecient (K-value) was calculate for each seperated chromatographic peak accroding to equation to find the best solvent condition for HPCPC separation.

K= [Area under the curve in top phase] / [Area under the curve in bottom phase]

2.22. Seperation of active compounds from SPEE by CPC

Centrifugal partition chomatography (CPC) was used to seperate the active compounds from SPEE. In this study, the solvent of H:EA:Me:W of 1:13:4:7 was used as the solvent system for seperation. The top phase was used as the mobile phase, whereas the bottom phase was used as the stationary phase. The column of CPC was initially filled with the top phase and the mobile phase was pumped into the column while the CPC column was rotating at a speed of 1000 rpm. The CPC was operated in the ascending mode with a flow rate of 2 ml/min and changed to descending mode after operation 300 min. A sample weight of 500 mg of SPEE was introduced in to the

column and the effluents were monitored using an UV detector at a wave length of 254 nm. The fractions from the CPC were collected in to text tubes using a fraction collector (Gilson FC 203 B).

2.23. Analysis of fractions collected by CPC using HPLC

The fractions collected by CPC were analyzed using HPLC. The dry samples of each fractions were dissolved in 500 μL methanol and analysed by HPLC. Volume of 10 μL of sample was injected to a SunFire 5μm 4.6 × 250 mm column (Waters, Ireland) and run at 1.0 mL/min flow rate using a gradient of ACN and D.W solvent system, 0-10 min: 20 % ACN and 80 % D.W, 10-40 min 25 % ACN and 75 % D.W, 40-50 min 100 % ACN and 0 % D.W, 50-60 min 100 % ACN and 0 % D.W and detected wave length was 290 nm. Sample fractions were pooled together.

2.24. NMR spectroscopy of the target compounds

The chemical structures of target compounds were analysed by the spectroscopic data given by the fourier-transform nuclear magnetic resonance spectroscopy. The magnetic properties ^{1}H isotope of hydrogen peroxide and ^{13}C isotope of carbon were used for nuclear magnetic resonance spectroscopy to record the spectrum. The ^{1}H and ^{13}C spectrums were recorded on JEOL DELTA-400 (400 Hz) spectrometer. Target compounds were dessolved in the deuterated MeOH, the chemical shift of the spectrum were reported as δ relative to tetramethylsilane as an internal standard.

2.25. Statistical analysis

The experiments were performed in triplicate. The data were expressed as the mean ± standard error (SE), and one-way ANOVA test (using SPSS 11.5 statistical software) was used to compare the mean values of each treatment. Significant differences between the means of parameters were determined by the student's *t*-test (* $p < 0.05$, ** $p < 0.001$).

3. Results and discussion

3.1. Sample extraction - 70% crude ethanol extract (SPE)

A weight of 10 g of lyophilized *Spirogyra* sp. powder was extracted by 70 % ethanol and filtered though Whatman No:4 filter paper. Then, the extracts were concentrated by rotary evaporator at a low pressure. A valume of 1 mL of 70 % ethanol extract was used to check the yield of extraction. The yield of extract was recorded as 19.33 ± 2.23 % (Table 1). The obtained crude extract was 19.28 g (SPE). SPE was stored at -20 ℃ in refrigerator until further use.

3.2. Total phenolic content of SPE

The total phenolic content of SPE was determined by the method described in 2.5. The result (Table.1) indicated that the phenolic content of SPE is 22.74 ± 1.03 %. The results suggests a higher phenolic content in SPE. Sugesting that the green algae *Spirogyra* sp. is rich in phenolic content. Normally, extracts rich in phenolic content indicates strong radical scavenging and antioxidant activities. These results suggests that SPE can be selected as a material for anti-aging research.

Table 1. The yield and total phenolic content of *Spirogyra* sp. 70% EtOH extract

Sample	SPE
Yield (%)	19.33± 2.23
Phenolic content (%)	22.74±1.03

3.3. Free radical and hydrogen peroxide scavenging activity of SPE

Many studies reportes that plants or seaweeds which have a high phenolic content which have a strong free radical scavenging activity. *Spirogyra* sp. is a freshwater microalgae, which contains a high phenolic content as reported by our provious study(Ji-Hyeok Lee, 2015). Accroding to the result of phenolic content analysis of SPE, we can guess that SPE will show a strong radical scavenging activity. Free radicals and hydrogen peroxide scavenging activity of SPE were deterimined by ESR and colorimetric method. The methods described at 2.6, 2.7, 2.8 and 2.9. The results shown as Fig. 3, Fig. 4, Fig. 5 and Fig. 6. The result suggest that SPE show a strong free radicals and hydrogen perxide scavenging activity, excepially DPPH radical scavenging activity. The IC_{50} values of DPPH, alkyl, hydroxyl radicals and hydrogen peroxide scavenging activities of SPE are 8.660 ± 0.295, 19.798 ± 1.931, 153.692 ± 16.081 and 85.425 ± 0.874 μg/mL respectively (Table 2). Those results suggest SPE have a strong free radicals and hydrogen peroxide scavenging activity.

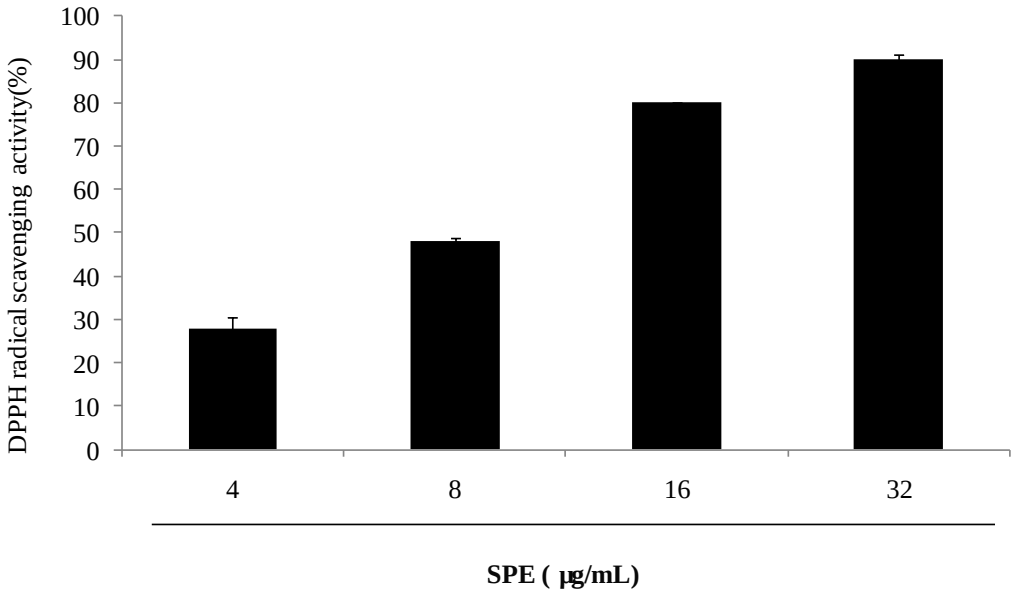

Fig. 3. DPPH radical scavenging activity of SPE. DPPH radical scavenging activity was determined by ESR. Experiments were performed in triplicate and the data are expressed as mean ± SE.

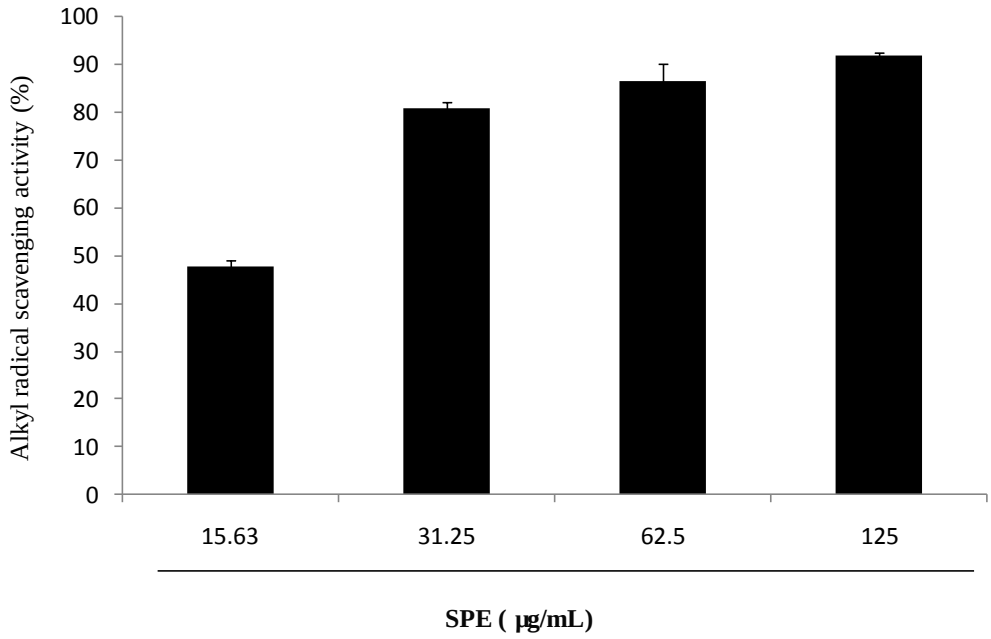

Fig. 4. Alkyl radical scavenging activity of SPE. Alkyl radical scavenging activity was determined by ESR. Experiments were performed in triplicate and the data are expressed as mean ± SE.

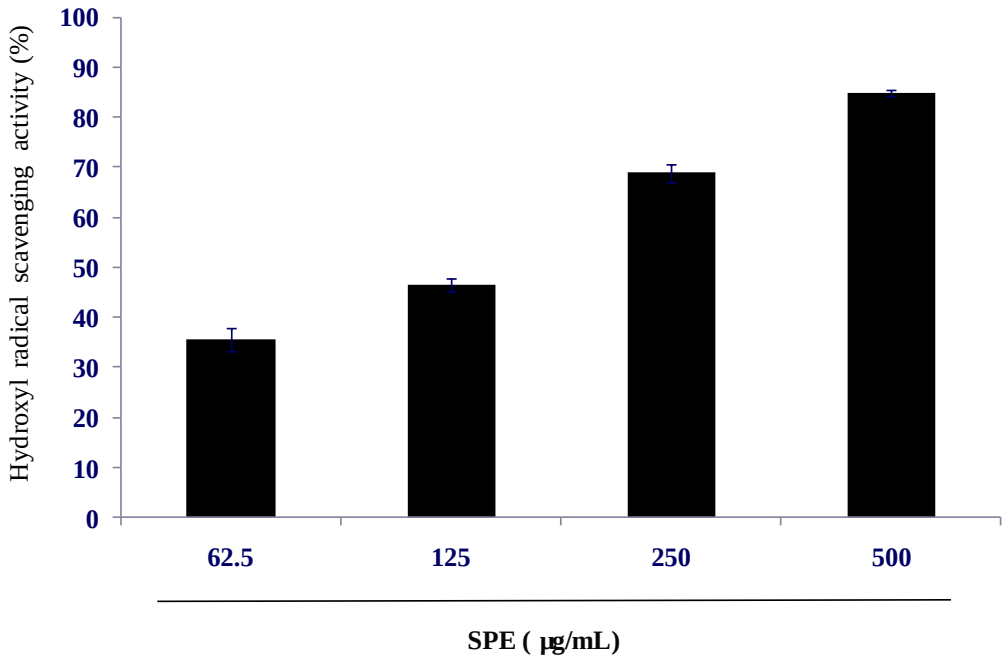

Fig. 5. Hydroxyl radical scavenging activity of SPE. Hydroxyl radical scavenging activity was determined by ESR. Experiments were performed in triplicate and the data are expressed as mean ± SE.

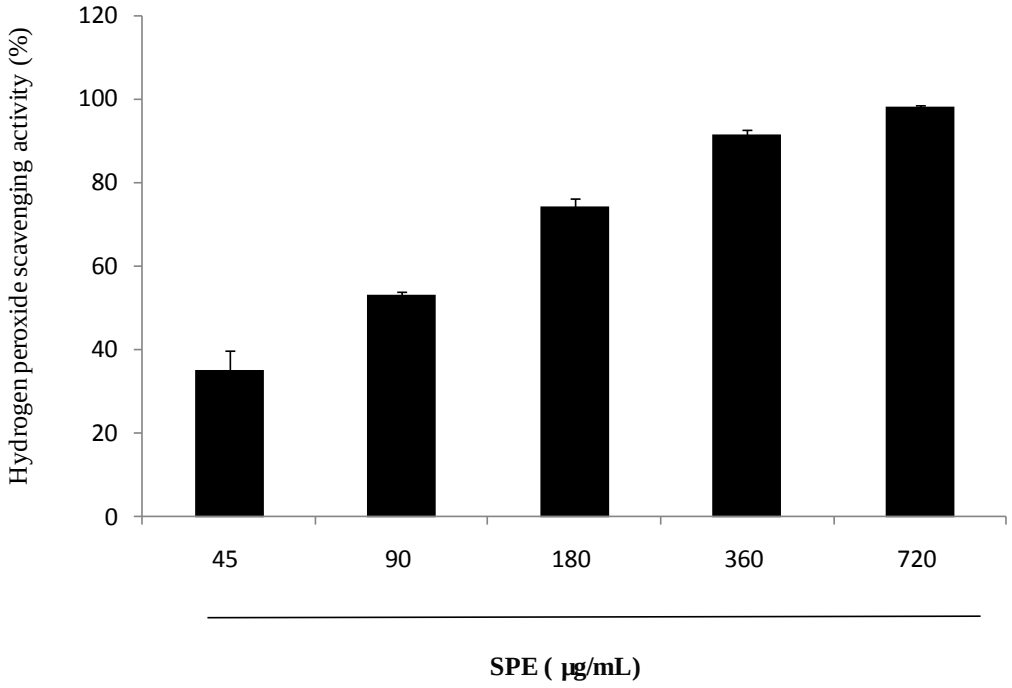

Fig. 6. Hydrogen peroxide scavenging activity of SPE. Hydrogen peroxide scavenging activity was determined by colorimetric method. Experiments were performed in triplicate and the data are expressed as mean ± SE.

Table 2. IC_{50} values of free radicals and hydrogen peroxide scavenging activities of SPE

Radical/Hydrogen peroxide	IC_{50} (μg/mL)
DPPH	8.660±0.295
Alkyl	19.798±1.931
Hydroxyl	153.692±16.081
Hydrogen peroxide	85.425 ± 0.874

3.4 . On-line HPLC analysis of SPE

On-line HPLC analysis of SPE was determined by the method described in 2.10. The chromatograph of online HPLC in Fig. 7 (A), there are 7 main peaks at the wave length of 220 nm shown as the chromatograph and named as peak-1, peak-2, peak-3, peak-4, peak-5, peak-6 and peak-7 respectively. The $ABTS^{+}$ absorbance curve was shown in Fig. 7 (B). According to the result, the peak area of peak-6 is higher than other pearks, It means that peak-6 is the main compound of SPE. The $ABTS^{+}$ absorbance of peak-6 is the strongest of this 7 peaks . It means that peak-6 shown the strongest ATBS radical scavenging activity of those 7 peaks. This result suggest that SPE has a strong ABTS radical scavenging activity and peak-6 is the main ABTS radical compound of SPE.

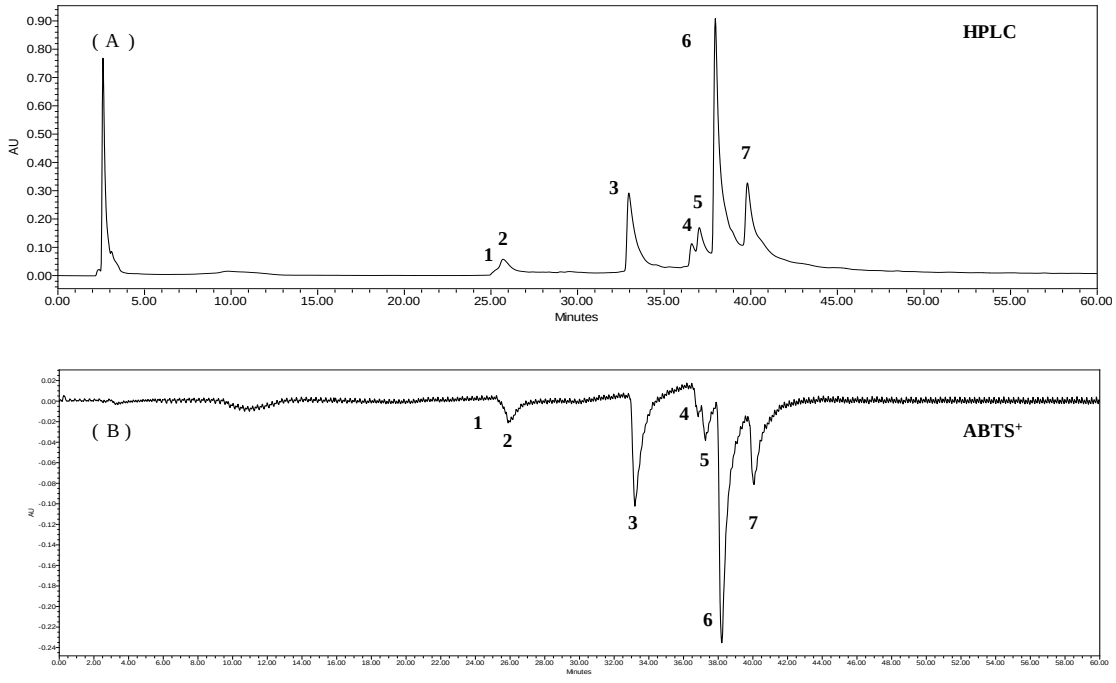

Fig. 7. On-line HPLC analysis of SPE. (A) HPLC chromatogram, (B) $ABTS^{+}$ absorption sepectrum. Colunm: Atalantis T3 3 μm ODS column (3.0 × 150 mm i.d.); mobile phase: acetonitrile-distilled water solvent system (0-10 min: 0:100 v/v; 10-30 min: 25:75 v/v ; 30-80 min: 50:50 v/v ; 80-90 min: 100:0 v/v; 90-110 min: 100:0 v/v); flow rate 0.3 mL/min ; detected wave length was 220 nm. ABTS solution eluted at flow rate 1.0 mL/min and measured as negative peak by UV/Vis detector at a wave length of 680 nm.

3.5. Cytotoxicity of SPE on HaCaT cells

It is necessary to analys cytotoxicity of sample before check bioactivity in vitro in cell lines. In this study, cytotoxicity of SPE was determinated by MTT analysis, the method described at 2.12. The cell viability of the cellsnot treated with SPE was considerd as 100 % viable. The cell viability of cells treated with SPE is shown as Fig. 8. The cell viability of the cells treated with 100 and 200 μg/mL of SPE were decreased with the concentration increasing. The cell viability of the cells treated with a final concentration of 200 μg/mL SPE is around 80%. It means that a high concentration of SPE has some toxicity for HaCaT cells. The cell viability were not decrased when the cells were treated with SPE below 50μg/mL. It means that the maximun safe concentration treatment to HaCaT cells of SPE is 50 μg/mL. So, 50 μg/mL of SPE was considered as hightest concentration treatment for HaCaT cells in futher research.

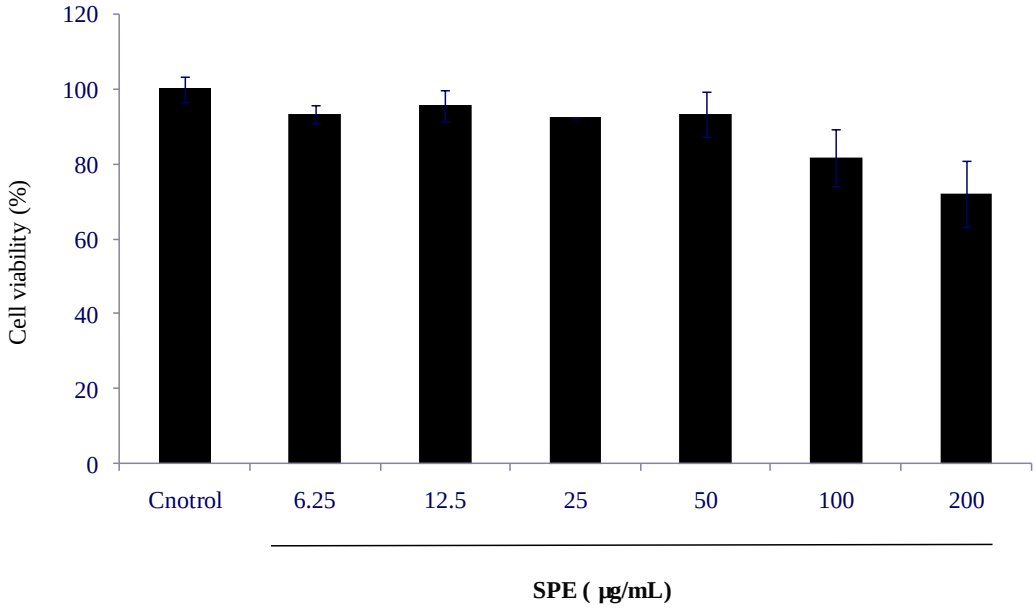

Fig. 8. Cell viability of HaCaT cells after treated SPE. HaCaT cells were seeded in 96-well plate at a concentration of 1.0 × 10^5 cells/mL. Cell viability was determined by MTT assay. Experiments were performed in triplicate and the data are expressed as mean ± SE.

3.6. Intracellular ROS scacvenging activity of SPE in HaCaT cells

Intracellular ROS scavenging activity of SPE was determined by DCF-DA analysis following the method discribed in 2.13. The results showed in Fig. 9. The cellular ROS generation were increased after UV-B irradiation without pretreated with SPEE compared with control. And the cellular ROS generation of the cells pretreated with a final SPE showed a siganificant dose dependent decreasing compared with the cells irradiated with UV-B only. The result suggest that SPE can scavenge or reduce ROS generation induced by UV-B irradiation.

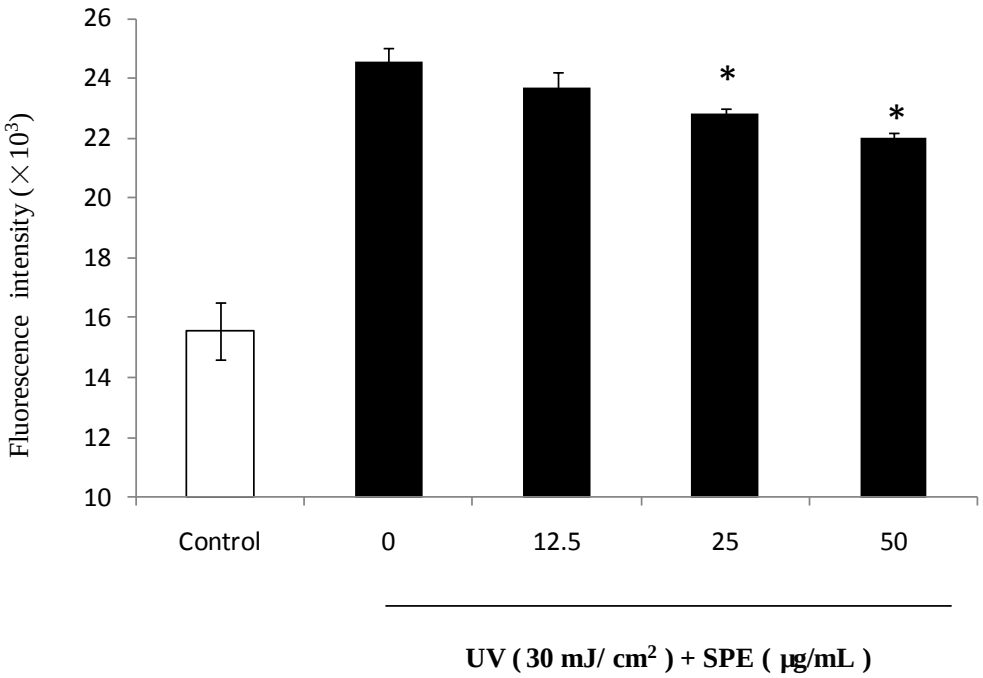

Fig. 9. Intracellular ROS scavenging activity of SPE in HaCaT cells, HaCaT cells were seeded into a 24-well plate at a concentration of 2.0 × 10^5 cells/mL. Cellular ROS level were determined by DCF-DA analysis. Experiments were performed in triplicates and the data are expressed as mean ± SE. * $p<0.05$.

3.7. Cytoprotective effect of SPE against UV-B irradiation in HaCaT cells

The cytoprotective effect of SPE was determined by LDH analysis and MTT analysis following the method discribed in 2.14. The result shown in Fig. 10. The LDH release of the cells (Fig. 10.(A)) without SPE pretreatment, increased and the cell viability (Fig. 10.(B)) were decreased after UV-B irradiation compared with control. The LDH resease level of the cells pretreated with a final concentrations of 25 and 50 μg/mL SPE showed a siganificant decrease compared with the cells irradiated with UV-B only. The cell viability of the cells pretreated with a final concentration 50 μg/mL SPE showed a siganificant increase compared to the cells irradiated with UV-B only.

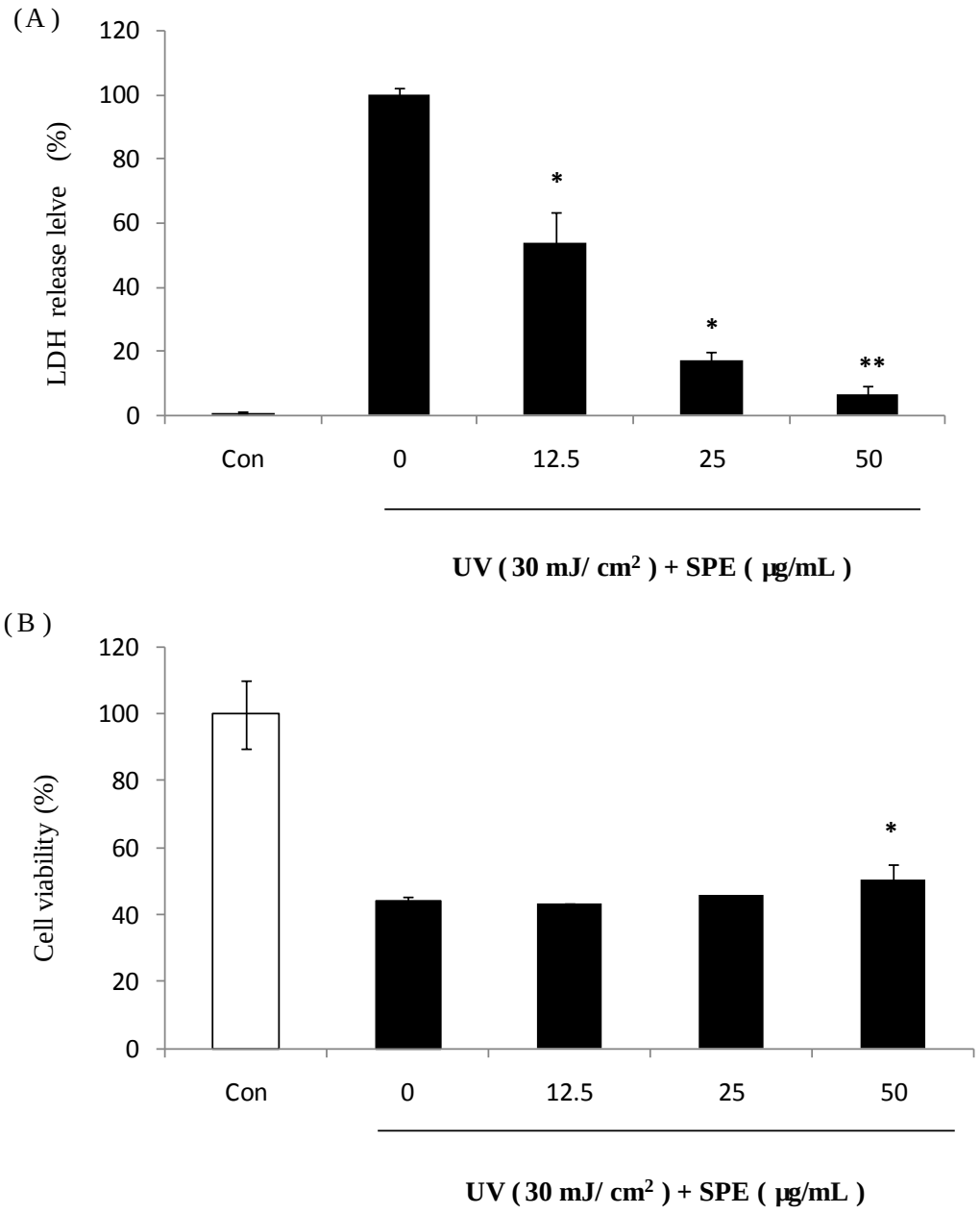

Fig. 10. Cytoprotective effect of SPE in HaCaT cells. HaCaT cells were seeded into a 24-well plate at a concentration of 2.0 × 10^5 cells/mL. Cell damage degree and viability were determined by LDH and MTT analysis. (A): LDH release level**,** (B): cell viability. Experiments were performed in triplicate and the data are expressed as mean ± SE. * $p<0.05$. ** $p<0.001$.

3.8. Fractionation of SPE using different solvents

The dry SPE sample was dissolved in D.W and fractionated by different organic solvents following the methed discribed in 2.15. Then, the 4 fractions were named as SPEH, SPEC, SPEE and SPEW. The weights of SPEH, SPEC, SPEE and SPEW were 37.5 mg, 154.3 mg, 524.6 mg and 1166 mg respectively (Fig. 11). The yield of each fraction of SPE is indicated in Table 3. The fractctions were stored at -20 ℃ in refrigerator until use.

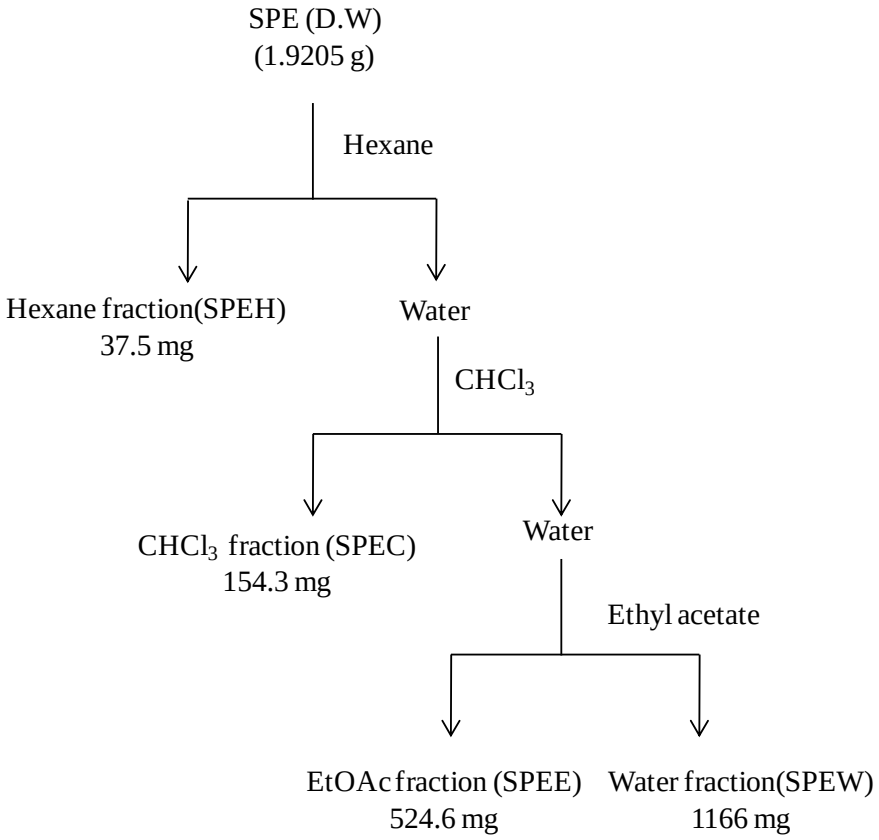

Fig. 11. The procedure of fractionation of SPE using different solvents. After fractionation, the 4 fractions were collected and named as SPEH, SPEC, SPEE and SPEW respectively.

3.9. Total phenolic contents of each fractions of SPE

The total phenolic content of each fractions of SPE were determined by the method described in 2.5 and compared with the total phenolic content of SPE. The result shown as Table 3. The total phenolic content of each fraction of SPE ranged between 7.44±0.52 % to 77.44±0.26 %. SPEH, SPEC, SPEW are contained a lower phenolic contents compared with SPE, and SPEE is contained the heightest phenolic content. SPEE was selected for further research as it contained the heightest phenolic levels.

Table 3. The yield and total phenolic content of each fractions of SPE

Sample	Yield (%)	Phenolicl content (%)
SPE	-	26.05 ± 0.52
SPEH	1.95	7.44 ± 0.78
SPEC	8.13	17.57 ± 0.00
SPEE	27.32	77.44 ± 0.26
SPEW	60.71	7.07 ± 0.26

3.10. Free radicals and hydrogen peroxide scavenging activities of SPEE

Free radicals and hydrogen peroxide scavenging activities of SPEE were deterimined by ESR and colorimetric methods as described in 2.6, 2.7, 2.8 and 2.9. The results shown in Fig. 12, Fig. 13, Fig. 14 and Fig. 15. The IC_{50} values of DPPH, alkyl, hydroxyl radicals and hydrogen peroxide scavenging activities of SPEE was 2.453 ± 0.107, 5.019 ± 0.208, 100.389 ± 12.419 and 24.546 ± 1.523 μg/mL respectively (Table 4). The free radicals and hydrogen peroxide scavenging activities of SPEE were stronger than SPE based on the IC_{50} values.

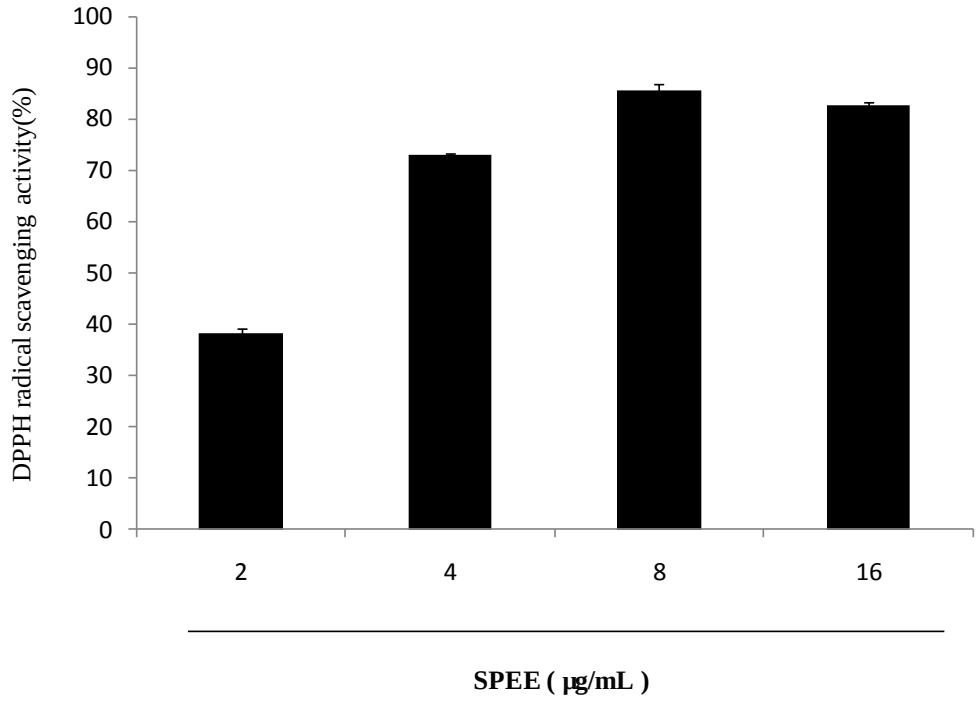

Fig. 12. DPPH radical scavenging activity of SPEE. DPPH radical scavenging activity was determined by ESR. Experiments were performed in triplicate and the data are expressed as mean ± SE.

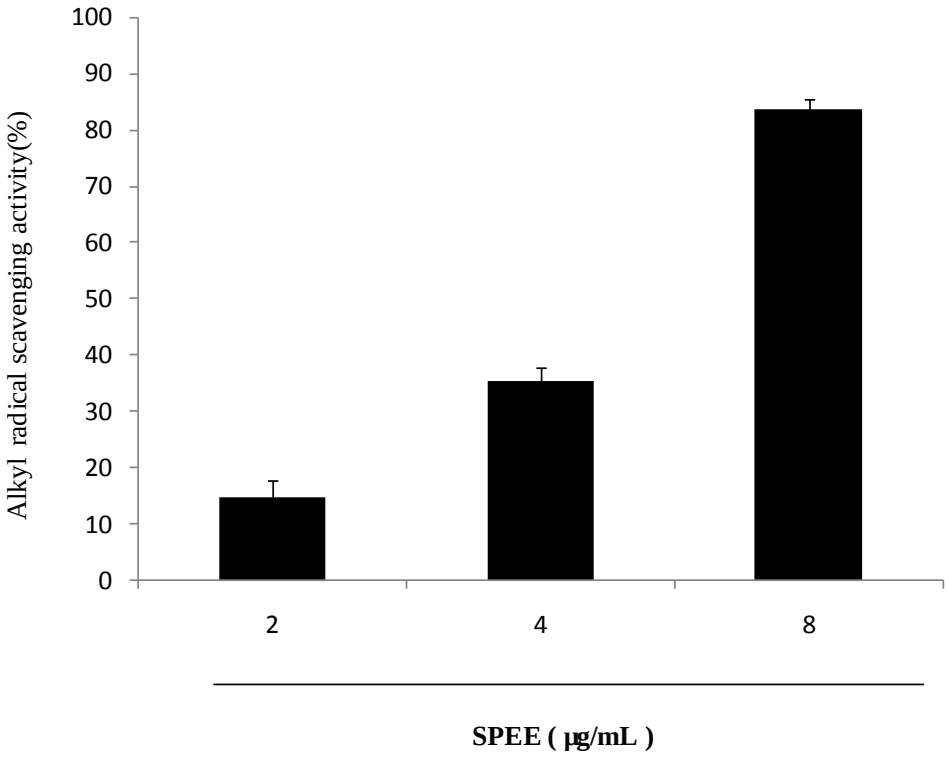

Fig. 13. Alkyl radical scavenging activity of SPEE. Alkyl radical scavenging activity was determined by ESR. Experiments were performed in triplicate and the data are expressed as mean ± SE.

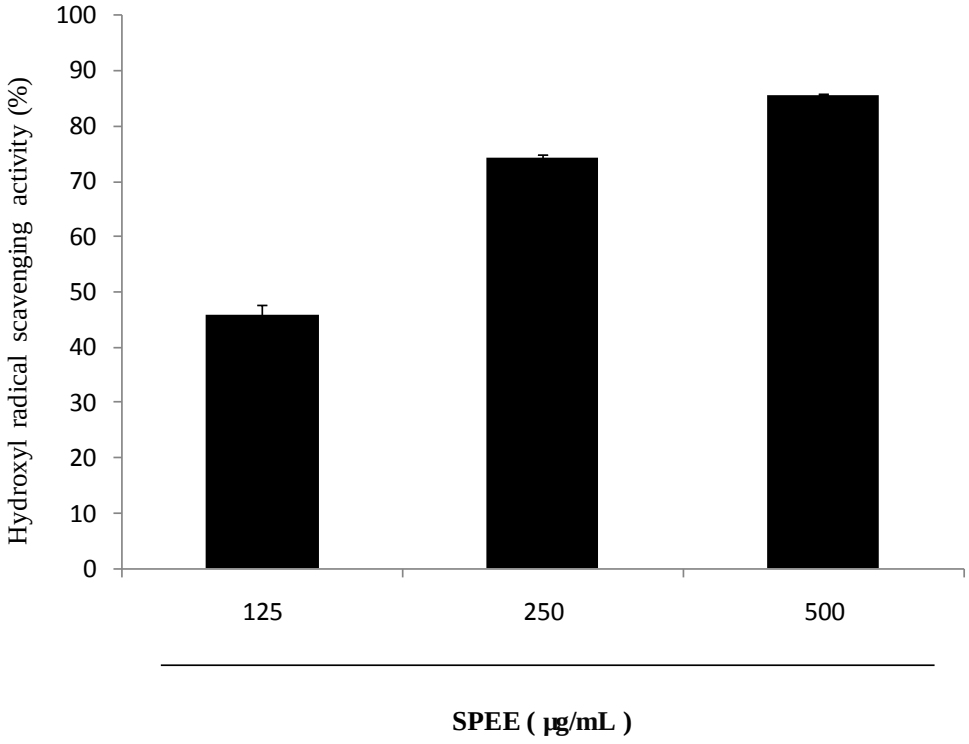

Fig. 14. Hydroxyl radical scavenging activity of SPEE. Hydroxyl radical scavenging activity was determined by ESR. Experiments were performed in triplicate and the data are expressed as mean ± SE.

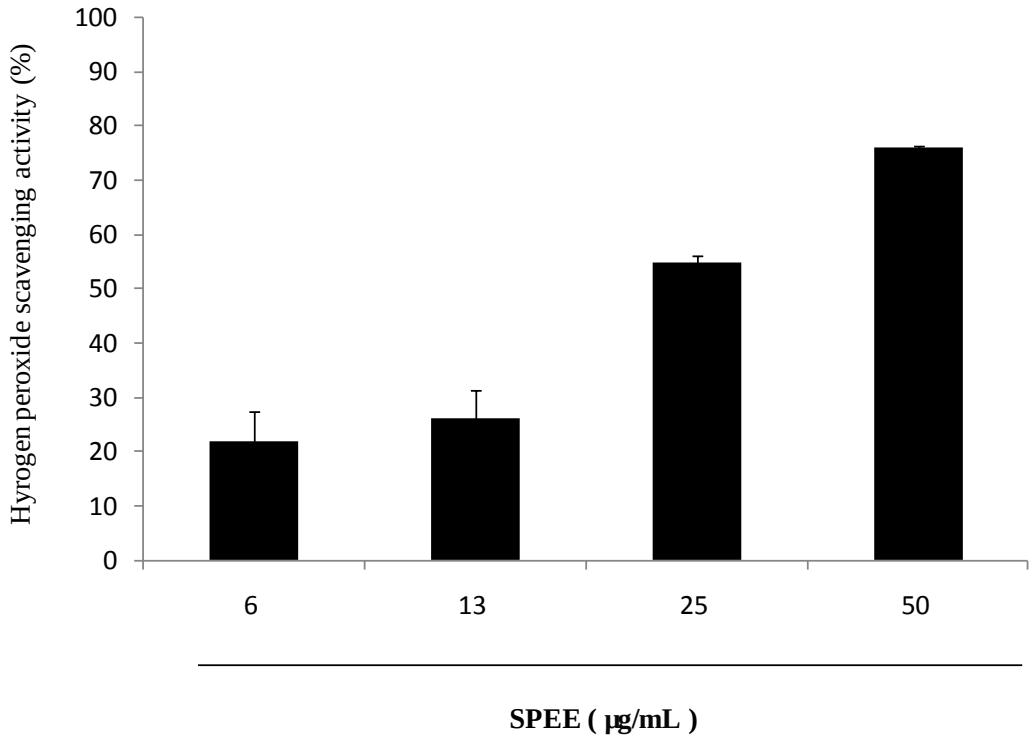

Fig. 15. Hydrogen peroxide scavenging activity of SPEE. Hydrogen peroxide scavenging activity was determined by colorimetic method. Experiments were performed in triplicate and the data are expressed as mean ± SE.

Table 4. IC_{50} values of free radicals and hydrogen peroxide scavenging activities of SPE and SPEE

Radical/Hydrogen peroxide	IC_{50} value (μg/ml)	
	SPE	SPEE
DPPH	8.660±0.295	2.453±0.107
Alkyl	19.798±1.931	5.019±0.208
Hydroxyl	153.692±16.081	100.389±12.419
Hygrogen peroxide	85.425 ± 0.874	24.546±1.523

3.11. On-line HPLC analysis of SPEE

On-line HPLC analysis of SPEE was determined by the method described in 2.16. Accordind to the chromatograph of online HPLC in Figure.16 (A), 8 main peaks were identified at the wave length of 290 nm. These will be named as peak-1, peak-2, peak-3, peak-4, peak-5, peak-6 , peak-7 and prak-8 respectively. According to the result, the peak areas of peak-6 and peak-8 are higher than other pearks, it means that peak-6 and peak-8 are main compounds of SPEE. The $ABTS^{+}$ absorbance curve is shown in Figure.16 (B). The $ABTS^{+}$ absorbance of peak-1 was identified as the one whith has the strongest intensity of all 8 peaks. It means that peak-1 shown the strongest ATBS radical scavenging activity of those 8 peaks. According to this results, peak-6 and peak-8 are two main compounds of SPEE, and peak-1 is show the strongest ATBS radical scavenging activity of those 8 peaks.

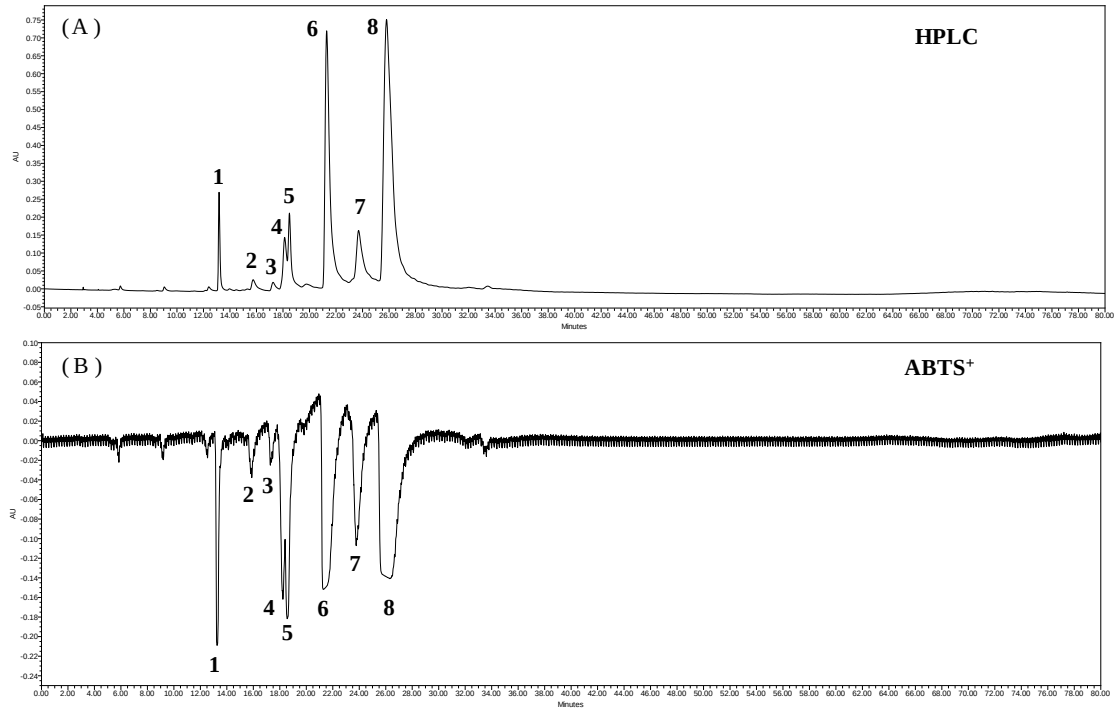

Fig. 16. On-line HPLC analysis of SPEE. (A) HPLC chromatogram, (B) $ABTS^{+}$ absorption sepectrum. Colunm: SunFire 5μm ODS column (4.6 × 250 mm i.d.); mobile phase: acetonitrile-distilled water solvent system(0-10 min: 20:80 v/v; 10-30 min: 25:75 v/v ; 30-50 min: 27:73 v/v ; 50-60 min: 30:70 v/v; 60-70 min:50:50 v/v; 70-80 min:100:0 v/v); flow rate 1.0 mL/min; detected wave length was 290 nm. ABTS solution eluted at flow rate 1.0 mL/min and measured as negative peak by UV/Vis detector at a wave length of 680 nm.

3.12. Cytotoxicity analysis of SPEE in HaCaT cells

The cytotoxicity of SPEE was determinated by MTT analysis according to the method described in 2.12. The cell viability was shown in Fig. 17. The cell viability of the cells treated with a final concentration of 6.25 and 100 μg/mL SPEE were not only decreased with the increasing concentrations, but inscreased dose dependently. Thus, 100 μg/mL was been thought as a safe concentration treatment for cells.

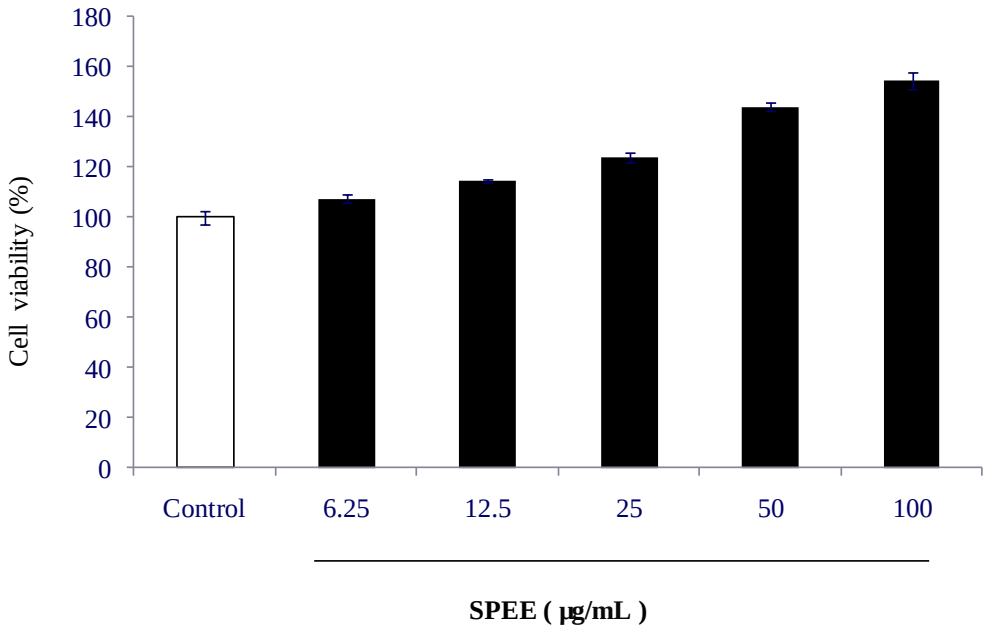

Fig. 17. Cytotoxicity analysis of SPEE. HaCaT cells were seeded in 96-well plate at a concentration of 1.0 × 10^5 cells/mL. Cell viability was determined by MTT assay. Experiments were performed in triplicate and the data are expressed as mean ± SE.

3.13. Intracellular ROS sacvenging activity of SPEE in HaCaT cells

Intracellular ROS scavenging activity of SPEE was determined by DCF-DA analysis following the method discribed in 2.13. The result shown in Fig. 18. The cellular ROS generation were increased after UV-B irradiation without pretreated with SPEE compared with control. The cellular ROS generation of the cells pretreated with a final concentration of 25 and 50 μg/mL. SPEE indicated a siganificant decrease compared with the cells irradiated with only UV-B.

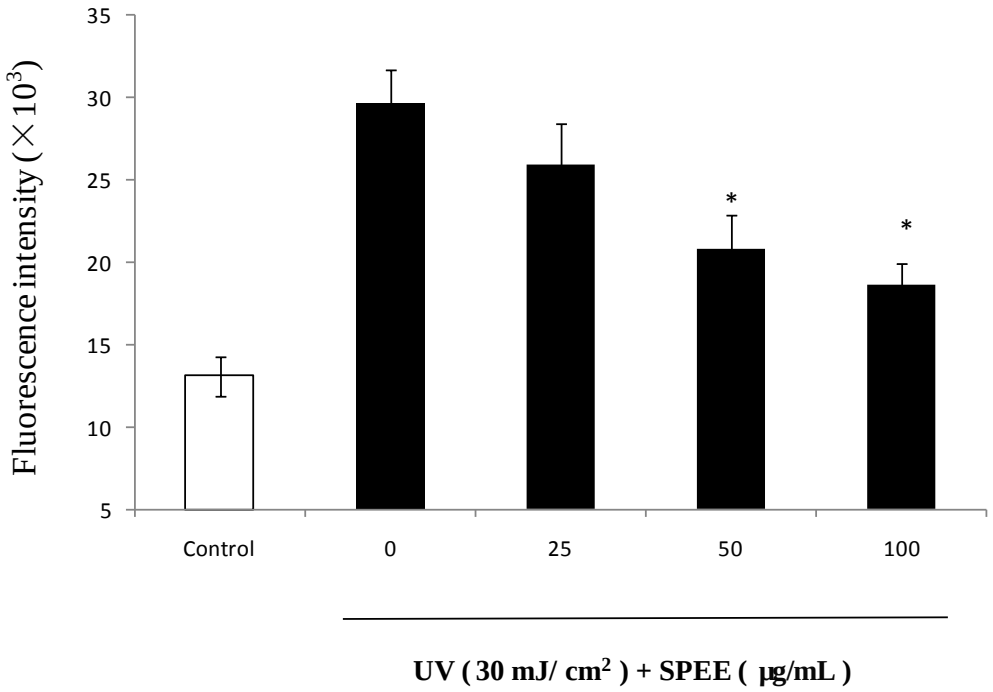

Fig. 18. Intracellular ROS sacvenging activity of SPEE in HaCaT cells. HaCaT cells were seeded in a 24-well plate at a concentration of 2.0 × 10^5 cells/mL. Cellular ROS level was determined by DCF-DA analysis. Experiments were performed in triplicate and the data are expressed as mean ± SE. * $p<0.05$.

3.14. Cytoprotective effect of SPEE against UV-B irradiation in HaCaT cells

The cytoprotective effect of SPEE was determined by LDH and MTT analysis following the method discribed in 2.14. The results in Fig. 19. indicates the LDH release levels of the cells (Fig. 19.(A) without SPEE pretreatement were increased and the cell viability (Fig. 19.(B) were decreased after UV-B irradiation compared with control. The LDH released level of the cells pretreated with SPEE indicates a dose dependent decrease compared with the cells irradiated with UV-B only. The cell viability of the cells pretreated with SPEE indicates a dose dependent increase compared with the cells irradiated with UV-B only.

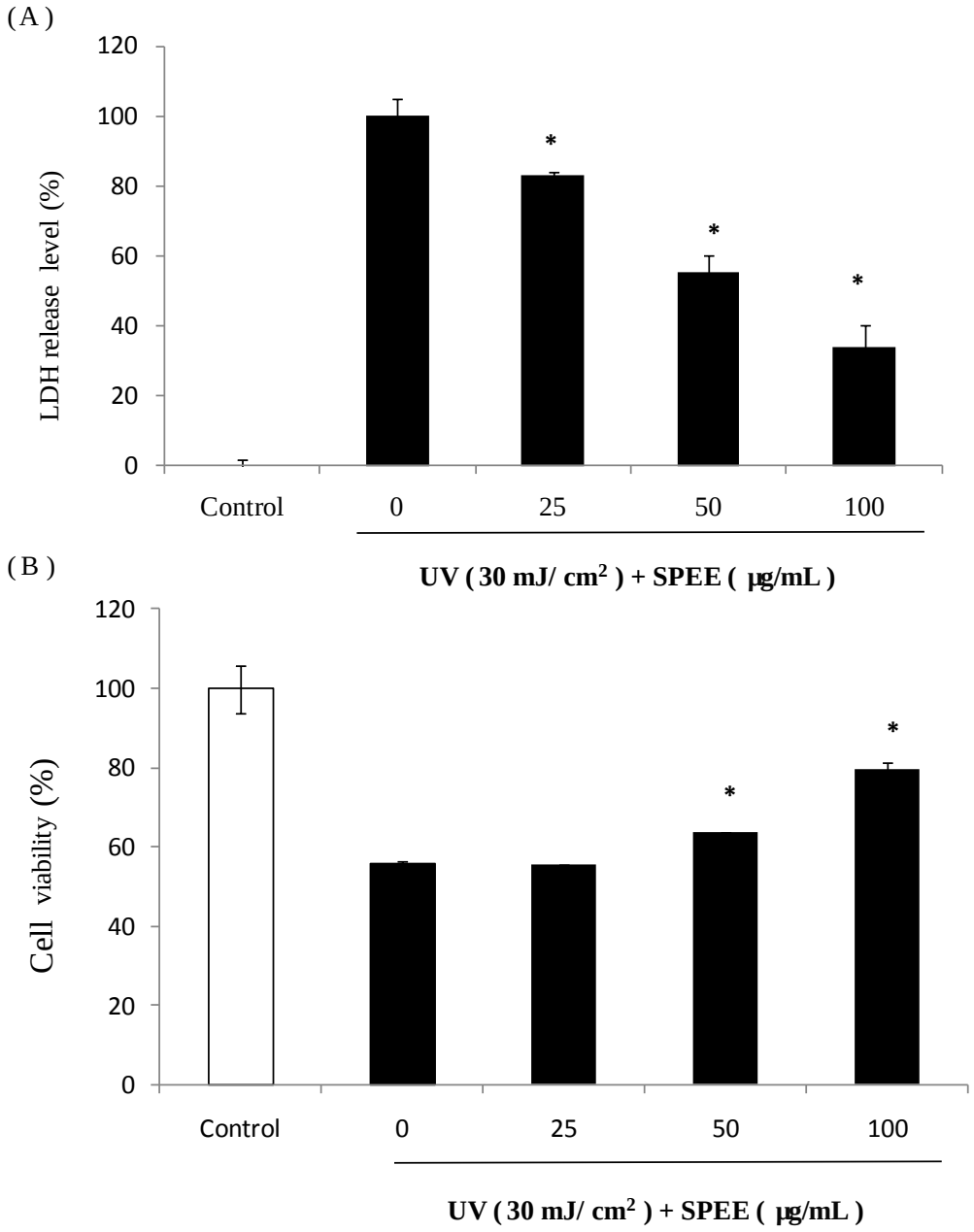

Fig. 19. Cytoprotective effect of SPEE in HaCaT cells. HaCaT cells were seeded in a 24-well plate at a concentration of 2.0 × 10^5 cells/mL. Cell damage degree and viability were determined by LDH and MTT analysis. (A): LDH release level**,** (B): cell viability. Experiments were performed in triplicate and the data are expressed as mean ± SE. * $p<0.05$.

3.15. Apoptotic body formation induced by UV-B irradiation in HaCaT cells

The cells were stained with Hoechest 33342 a cell permeable DNA dye. Then the nuclear morphology of cells were examined by fluorsence microscopy. The cell images were shown in Fig. 17. Accroding to the results, the amount of apoptotic bodies of the cells pretreated with SPEE increased with increasing concentrations of the sample compared with the cells irradiated by UV-B only. It means that SPEE can reduce cell apoptotic induced by UV-B irradiation.

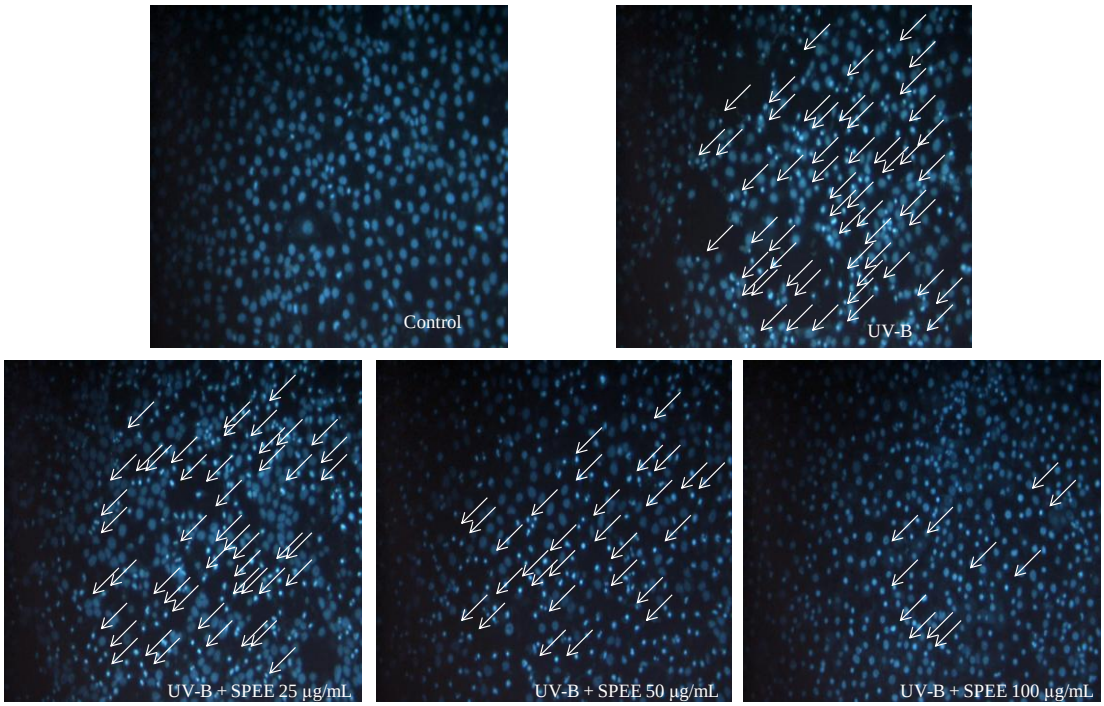

Fig. 20. Apototic body formation under UV-B irradiation. HaCaT cells were seeded in a 24-well plate at a concentration of 2.0×10^5 cells/mL. After 24 h incubation cells were pretreated with sample. After 2 h incubation, cells were exposed to 30 mJ/cm^2 UV-B and incubated 6 h. After incubation, cells were stained with Hoechest 33342, then, the nuclear morphology of cells were examined by microscope.

3.16. Cell cycle analysis

Cell cycle analysis was performed according to the methods described in 2.18. The results are indicated in Fig. 20. The DNA content analyses conducted following UV-B irradiation of HaCaT cells revealed an increase in the proportion of cells in sub-G_1 with a DNA content of 42.1 %. The sub-G_1 DNA content of the cells decreased dose dependently with the cells pretreated with different concentrations of SPEE solution.

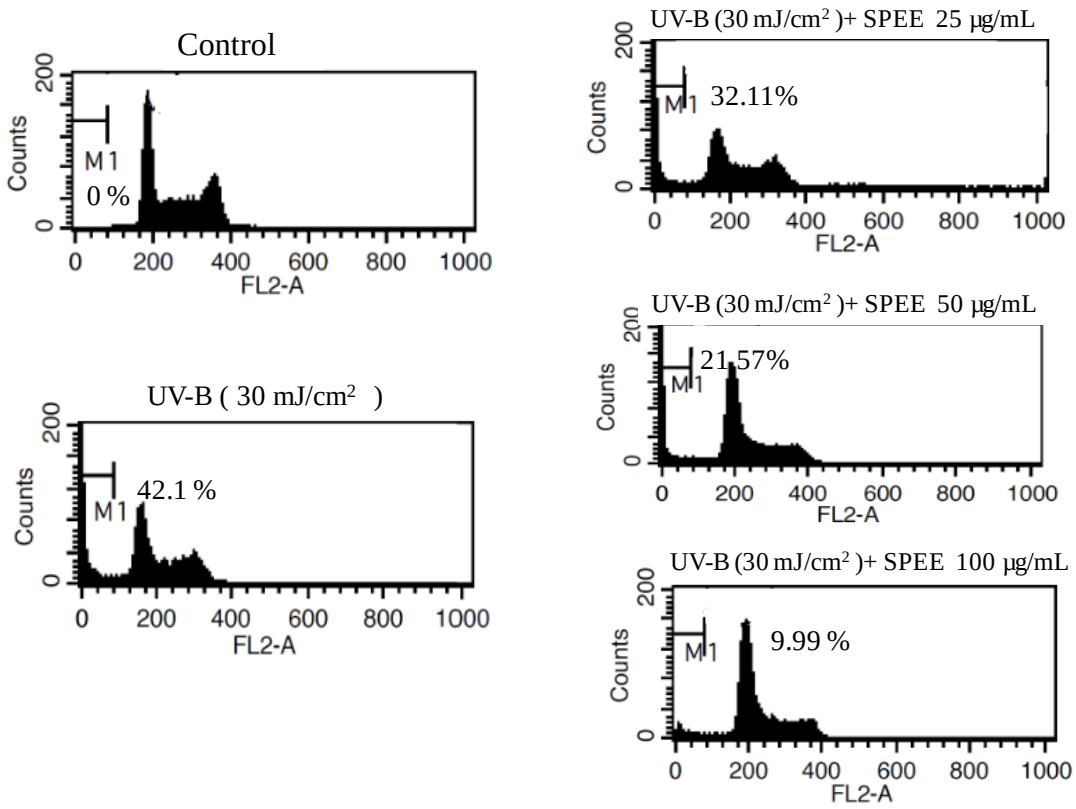

Fig. 21. Cell cycle analysis. HaCaT cells were seeded in a 24-well plate at a concentration of 2.0 × 10^5 cells/mL. After 24 h incubation cells were pretreated with sample. After 2 h incubation, cell were exposed to 30 mJ/cm^2 UV-B and incubated 6 h. After incubation, cells were collected and fixed by 70 % ethanol, Then the cells were incubated in dark with 1 mL EDTA which contained 100 μg PI and 100 μg Rnase A for 30 min at 37 ℃. Cell cycle analysis was conducted with FACS calibur flow cytometer.

3.17. Determination of ROS generation induced by UV-B irradiation in zebrafish

The UV-B protective effect of SPEE was determined using zebrafish model following the method described in 2.20. The result was shown in Fig. 22. The photographs were shown in Fig. 22 (A). According to the results, the fluorescence intensities decreased compared to UV-B treated group with a dose dependent (Fig. 22 (B)). This result suggests that a phenolic rich fraction seperated from *spirogyra* sp. indicates *in vivo* ROS scavenging activity.

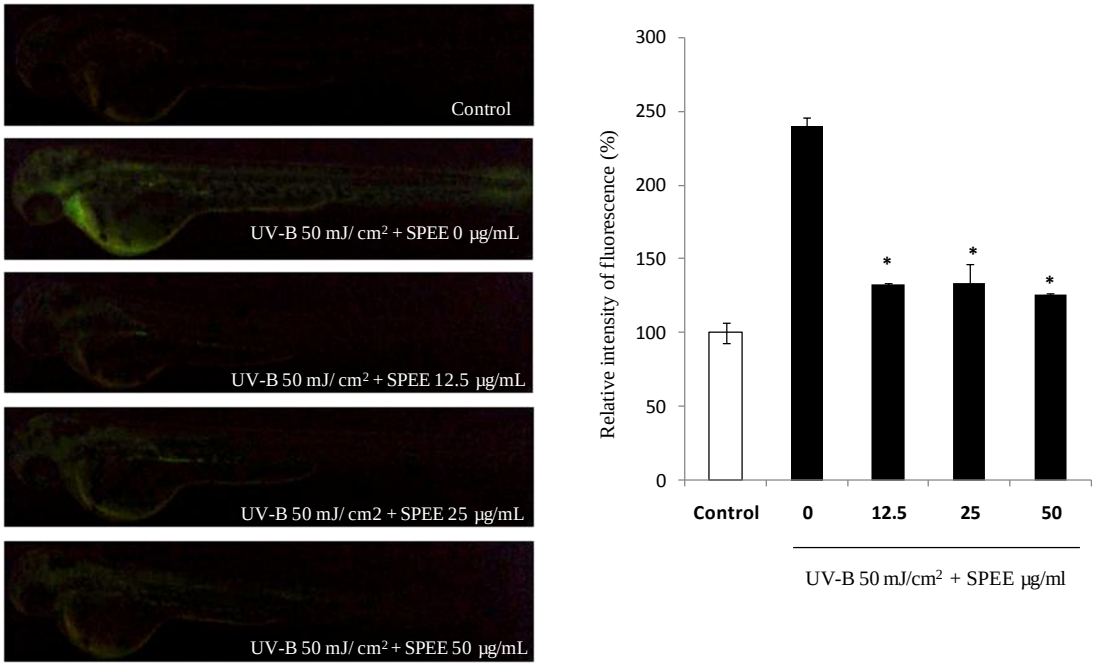

Fig. 22. ROS generation in SPEE pre-treated zebrafish. The 2 dpf zebrafish embryos were used for the anti-UV-B study. At 2 dpf, the embryos were treated with sample. After 1 hour, the embryos were exposed to 50 mJ/cm^2 UV-B per individual. After irradiating with UV-B, the embryos were treated with DCFH-DA solution (20 μg/mL) and incubated for 1 hour in the dark at 28.5℃. After anesthetized, the embyros were photographed under the microscope. The individual zebrafish larvae fluorescence intensity was quantified using an image J program. (A): The phptograph under fluorescence microscop, (B): The level of ROS generation in zebrafish. Experiments were performed in triplicates and data were expressed as mean ± SE. * $p<0.05$.

3.18. Optimisation of the Centrifugal Partition Chromatographic solvent system

The solvent system of CPC was optimised by HPLC following the method described in 2.21. The results shown in Fig. 23 and Table 5. The HPLC chromatograph of SPEE was shown in Fig. 23. The K-valve of each peak of each solvent system were calculated base on the areas under the peaks. The peak areas and K-value were shown in Table 5.

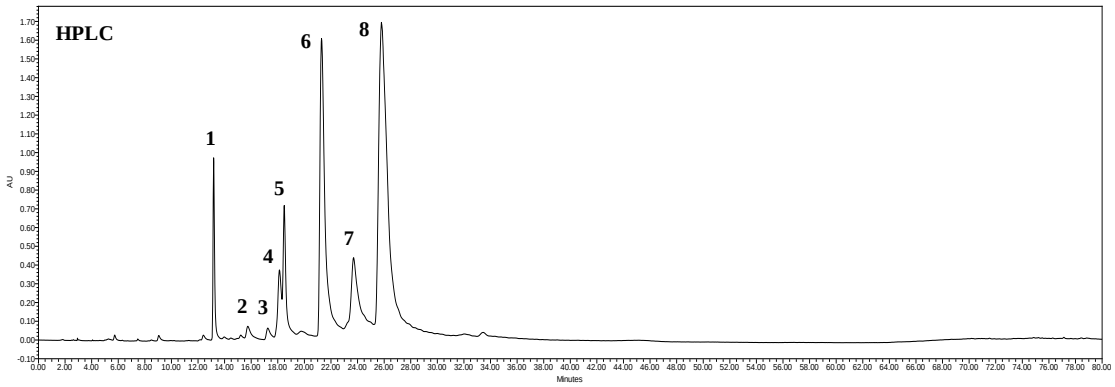

Fig. 23. The HPLC chromatogram of SPEE. Colunm: SunFire 5μm ODS column (4.6 × 250 mm i.d.); mobile phase: acetonitrile-distilled water solvent system(0-10 min: 20:80 v/v; 10-30 min: 25:75 v/v ; 30-50 min: 27:73 v/v ; 50-60 min: 30:70 v/v; 60-70 min:50:50 v/v; 70-80 min:100:0 v/v); flow rate 1.0 mL/min; detected wave length was 290 nm.

Table 5. Determination of partition coefficent of each and every peak appear in HPLC chromatogram between top phase and bottom phase of different types of CPC solvent system

H:E:M:W	1	2	3	4	5	6	7	8
1:12:4:7-T	956984	81339	45508	234401	1228818	1738793	869288	3191607
1:12:4:7-B	531870	133673	87615	438058	758992	3892181	1255285	5260706
T/B	1.799281779	0.6084924	0.519409	0.535091	1.619013	0.44674	0.692502	0.606687962
1:13:4:7-T	1056913	75778	50359	302867	1463001	2293957	924838	5214113
1:13:4:7-B	529094	144638	72191	-	1065361	3502341	700958	4161095
T/B	1.99759022	0.5239149	0.69758	-	1.65753	0.654978	1.319391	1.253062715

3.19. Seperation bioactivity compounds from SPEE by CPC

Accroding to K-value results, a solvent system of a ratio is 1:13:4:7 of H:EA:Me:W was used as the solvent system to separate the bioactivity compounds using CPC. The methods were discribed in 2.22 and the CPC chromatogram was shown in Fig. 24. The fractions were collected in test tubes by automatic sample collector and the analysis was performed by HPLC.

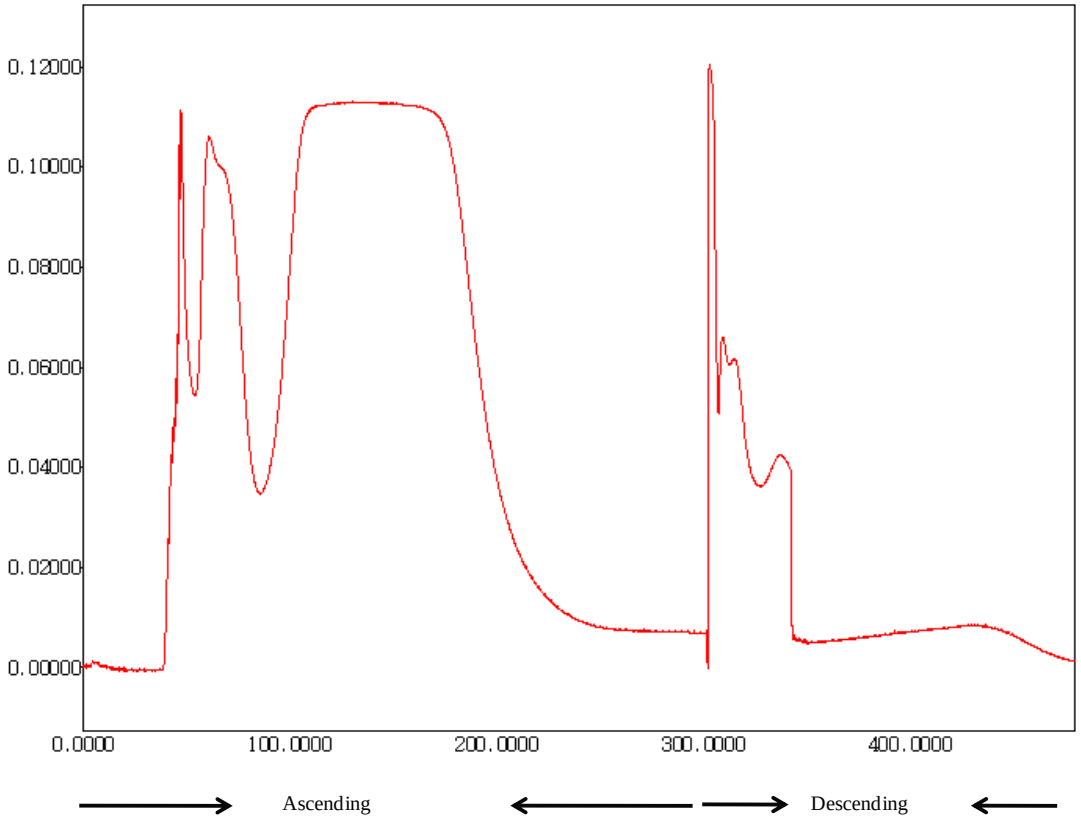

Fig. 24. The CPC chromatogram of SPEE. Solvent condition: stationary phase, bottom aqueous; mobile phase, top organic phase; rotation speed: 1000 rpm; flow rate: 2 mL/min; sample: a weight of 500 mg of sample dissolved in 6 mL misture of top and bottom phases (1:1,v/v) of the solvent system; UV detector at a wave length of 254 nm; fractions from the CPC were collected in to text tubes using a fraction collector.

3.20. Analysis of the fractions collected by CPC using HPLC

The fractions of SPEE seperated by CPC and collected into test tubes were analysed by HPLC. Comparing HPLC chromatographs of SPEE (Fig. 25 (A)) with our previous research (Ji-Hyeok Lee et al, 2015), peak-1 and peak-8 were gallic acid and methyl gallate respectively (Fig. 26). The same fractions were combine in one, then get 7 tragets, the chromatograph are shown in Fig. 25. The purity of the traget-1, traget-2, traget-3 and traget-5 were highter than the other tragets, which can be selected as the main tragets for further research.

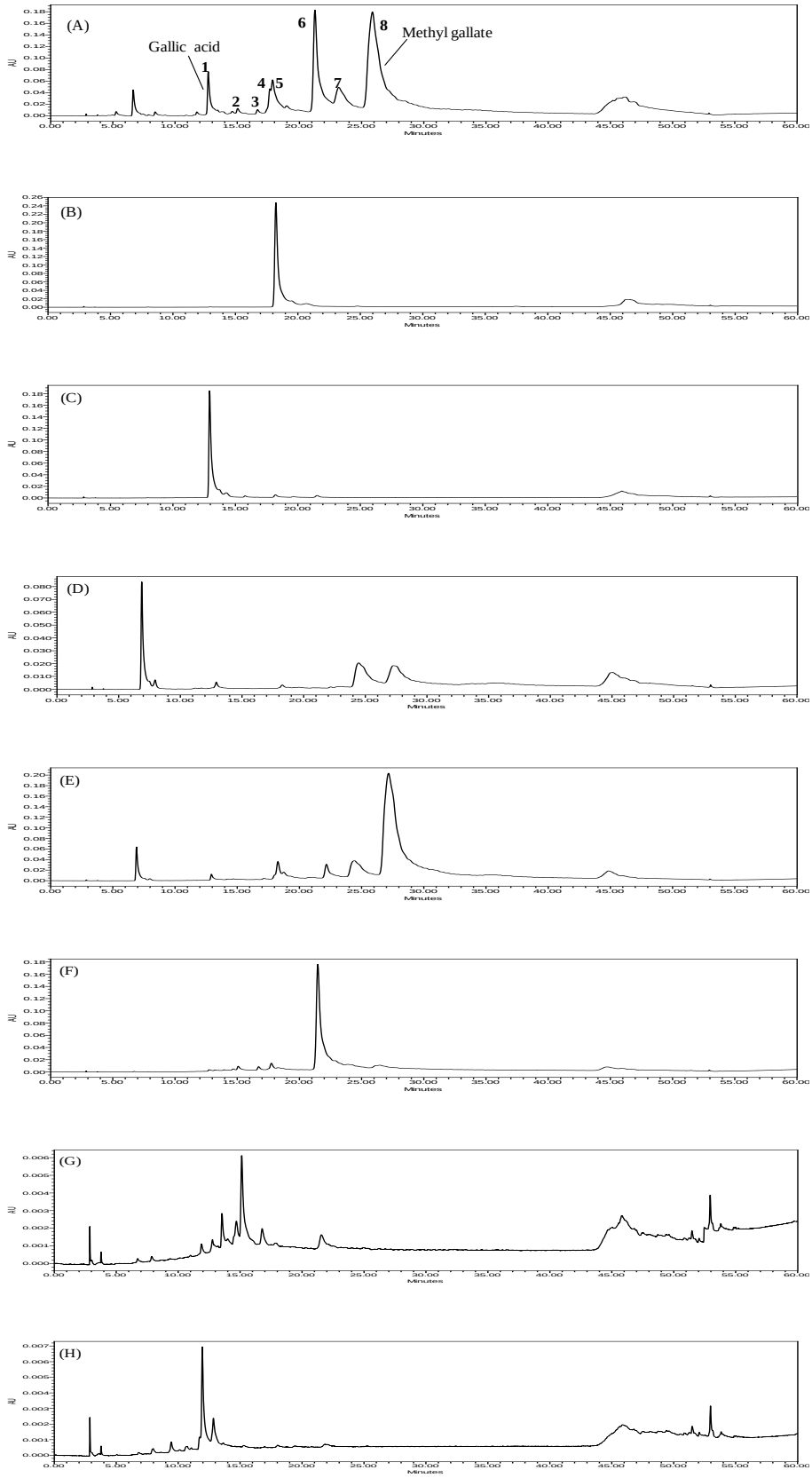

Fig. 25. Analysis of the fractions collected by CPC using HPLC (A) SPEE, (B) traget-1,(C) traget-2, (D) traget-3, (E) traget-4, (F) traget-5, (G) traget-6, (H) traget-7.

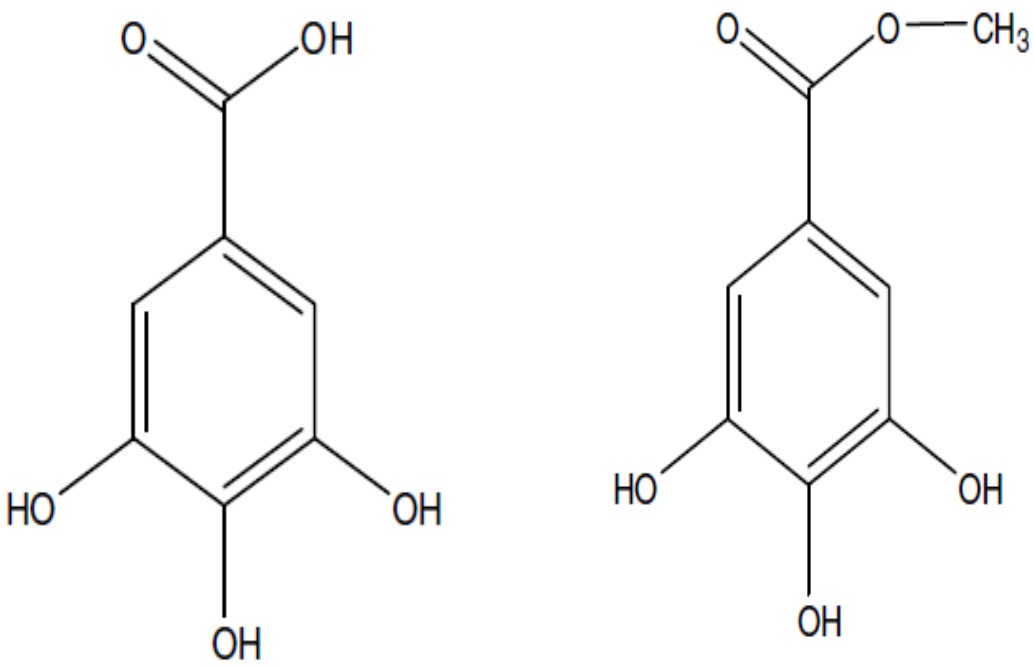

(A) (B)

Fig. 26. The chemical structure of gallic acid and methyl gallate. (A) Gallic acid, (B) methyl gallate.

3.21. Free radicals and hydrogen peroxide scavenging activities of the tragets fractions collected by CPC.

The free radical and hydrogen peroxide scavenging activities of the tragets collected by CPC were deterimined by ESR and using colorimetic methods as described in 2.6, 2.7, 2.8 and 2.9. The results shown inFig. 27, Fig. 28, Fig. 29 and Fig. 30. The IC_{50} values for DPPH, alkyl, hydroxyl radicals and hydrogen peroxide scavenging activities are shown in Table 6.

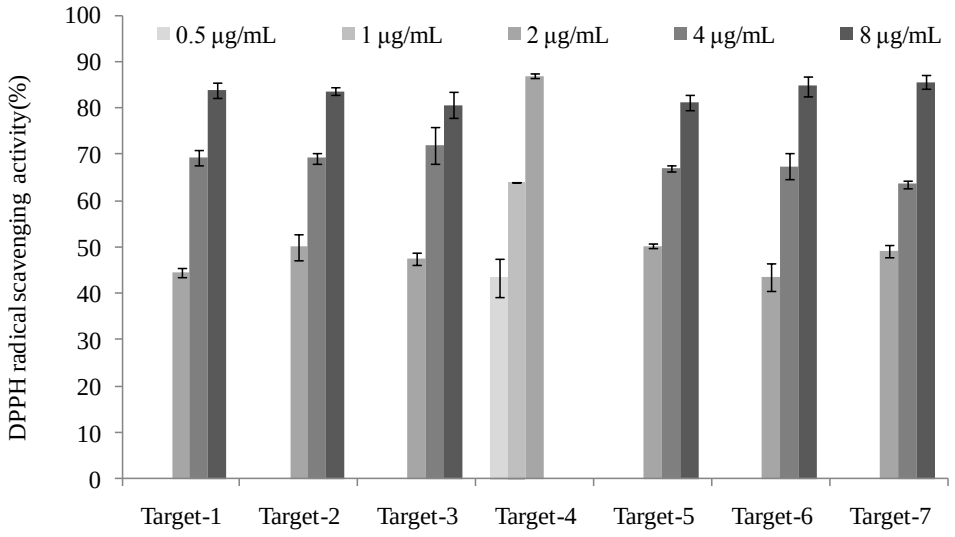

Fig. 27. DPPH radical scavenging activity of SPE. DPPH radical scavenging activity was determined by ESR. Experiments were performed in triplicates and data are expressed as mean ± SE.

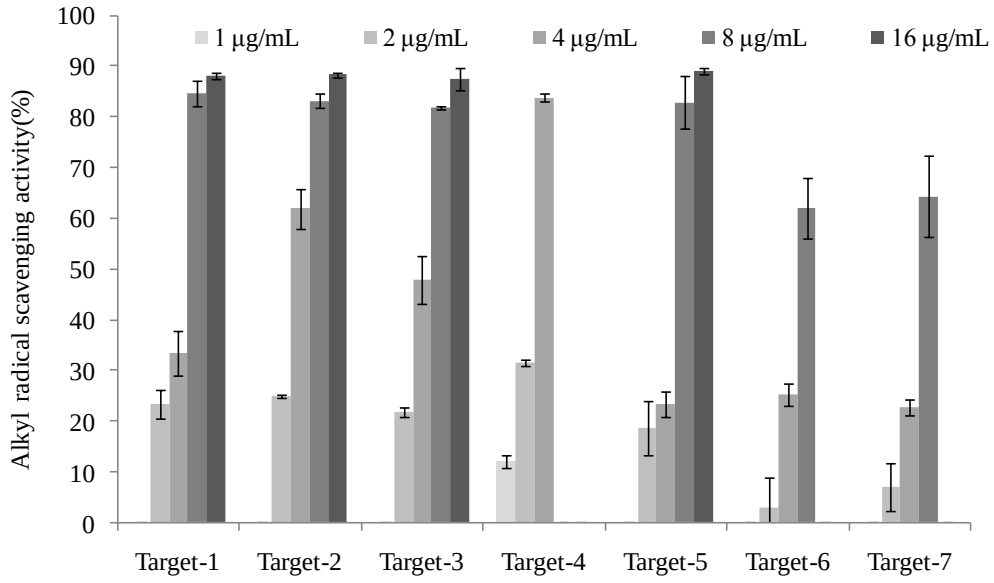

Fig. 28. Alkyl radical scavenging activity of SPE. Alkyl radical scavenging activity was determined by ESR. Experiments were performed in triplicates and the data are expressed as mean ± SE.

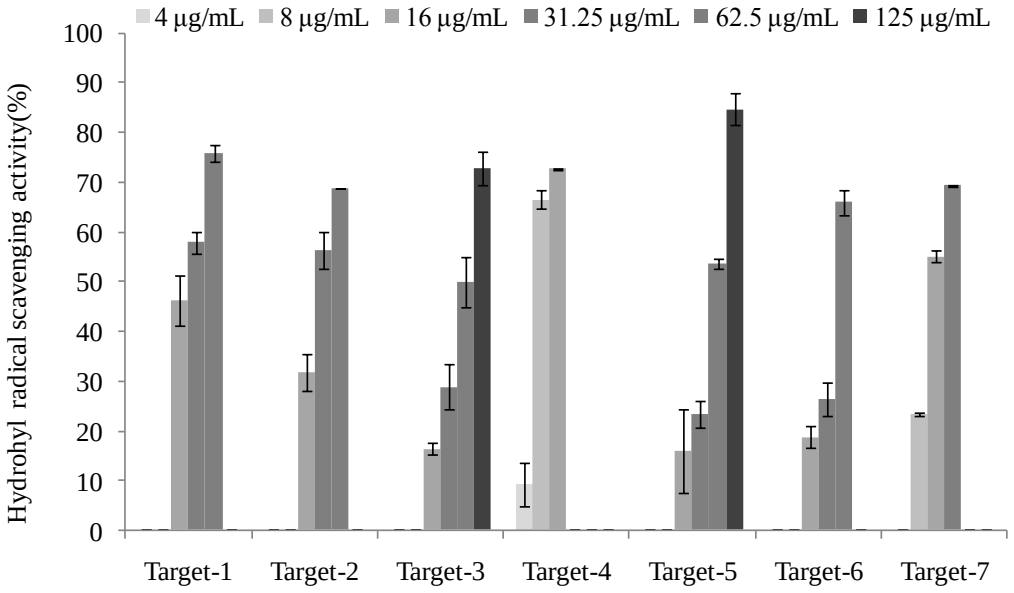

Fig. 29. Hydroxyl radical scavenging activity of SPE. Hydroxyl radical scavenging activity was determined by ESR. Experiments were performed in triplicate and the data are expressed as mean ± SE.

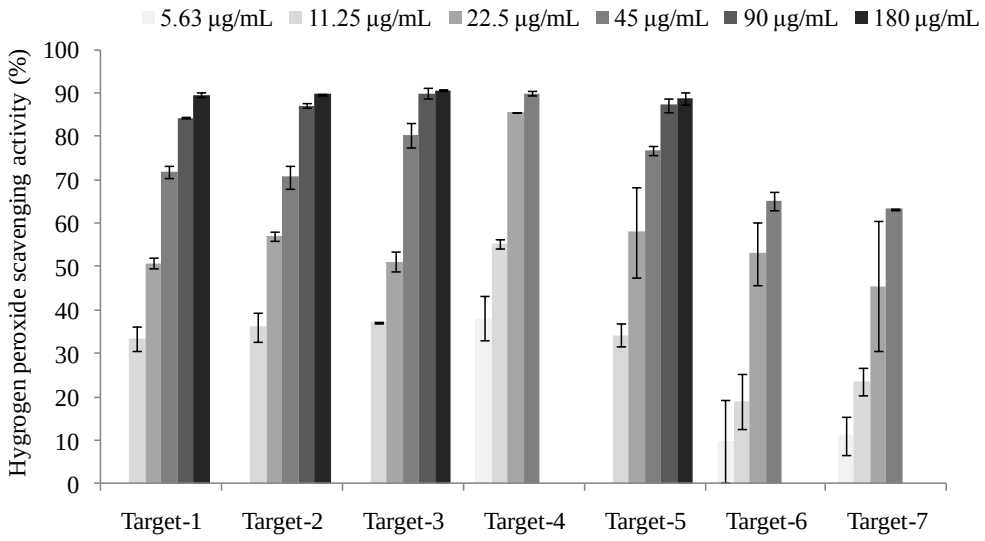

Fig. 30. Hydrogen peroxide scavenging activity of SPE. Hydrogen peroxide scavenging activity was determined by colorimetric method. Experiments were performed in triplicate and the data are expressed as mean ± SE.

Table 6. IC_{50} values of free radicals and hydrogen peroxide scavenging activities of the tragets fractions collected by CPC.

Target	IC_{50} (μg/mL)			
	DPPH	Alkyl	Hydroxyl	Hydrogen peroxide
Target-1	2.205±0.178	5.025±0.298	20.092±6.563	24.169 ± 0.979
Target-2	1.307±0.478	3.841±0.195	33.129±3.870	21.223 ± 0.706
Target-3	1.333±0.424	4.503±0.204	74.555±7.286	21.201 ± 0.172
Target-4	0.624 ± 0.087	2.469 ± 0.024	6.678±0.170	7.177 ± 2.297
Target-5	1.356±0.057	5.284±0.379	67.222±5.522	20.496 ± 4.045
Target-6	2.254 ± 0.455	6.553 ± 0.488	48.914±2.537	25.019 ± 6.581
Target-7	1.928 ± 0.180	6.459 ± 0.624	18.614±0.101	31.703 ± 3.776

3.22.NMR spectroscopy of the target compound

According to free radicals scavenging activities and the purity of each target. Target-1 was selected for the NMR analysis. The proton NMR spectrum and C-13 NMR spectrum for target-1 was obtained to analyse it's chemical structure. The proton NMR spectrum and C-13 NMR spectrum of traget-1 are shown in Fig. 31 and Fig. 32. According to the proton and C-13 NMR spectra, the compound could be identified as a phenolic compound. But futher studies are in need for the identification of the chemical structure of this compound.

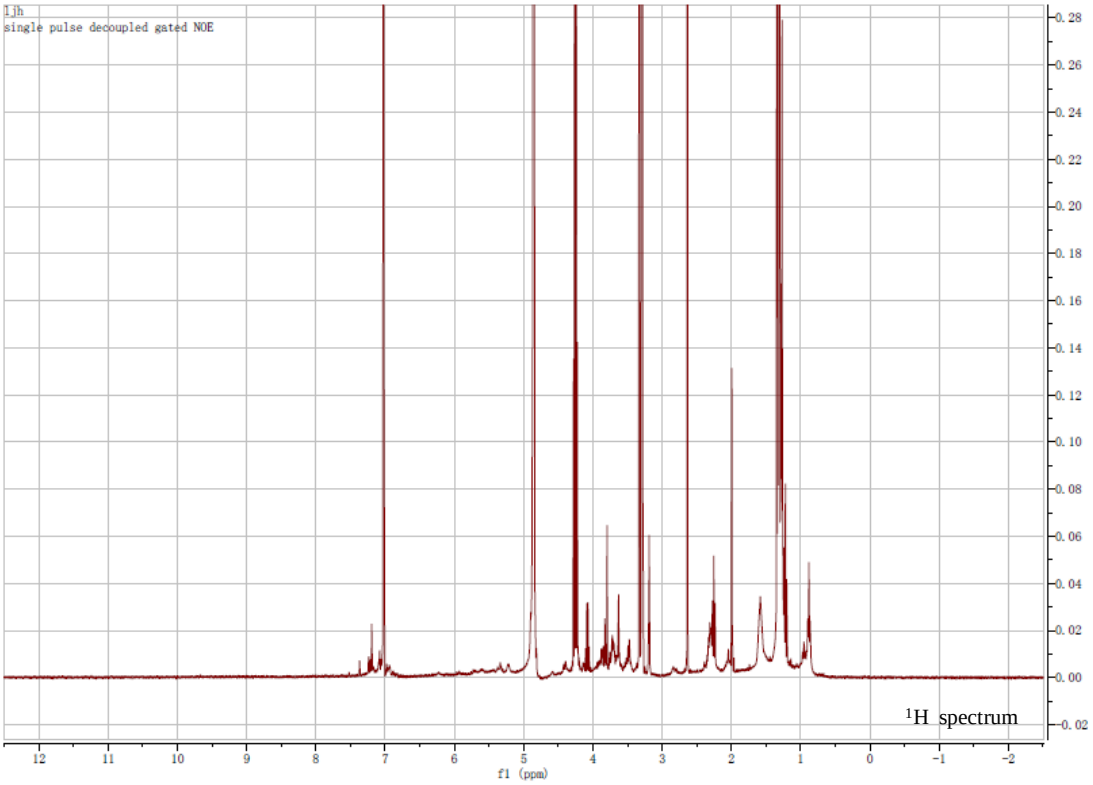

Fig. 31. Proton NMR spectrum of traget-1.

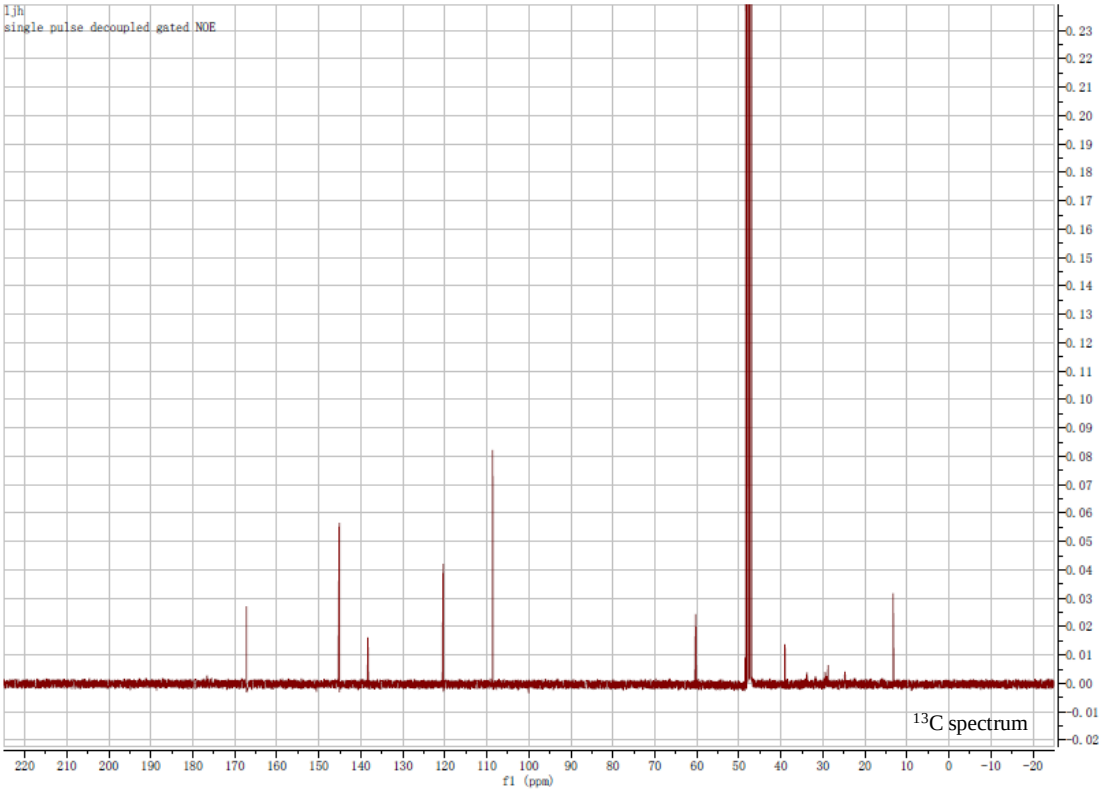

Fig. 32. ^{13}C NMR spectrum of traget-1.

4. Conclusion

In this study, a frashwater algea *Spirogyra* sp. was used as a material to evaluate anti-aging activity and to seperate active compounds. Regarding the observed results, the fresh water microalgea *Spirogyra* sp. is rich in natural phenolic compounds with a strong radical scavenging activity and UV-B protective effects. Finally it can be concluded that these compounds have the potential to be used as promising ingredients in cosmetic industry.

References

A. Kammeyer, R.M.Luiten. (2015). Oxidation events and skin aging,Ageing Research Reviews, 21, 16–29

Chandler, S.F., Dodds, J.H. (1983). The effect of phosphate, nitrogen and sucrose on the production of phenolics and solanidine in callus cultures of Solanum laciniatum. Plant Cell Reports, 2,105–110.

E.Herrero, J.Ros, G.Bell, E.Cabiscol. (2008) Redox control and oxidative stress in yeast cells. Biochim. Biophys. Acta: Gen.Subj.1780, 1217–1235.

Fuad Salem Eshaq , Mir Naiman Ali, Mazharuddin Khan Mohd. (2010) *Spirogyra* biomass a renewable source for biofuel (bioethanol) Production. International Journal of Engineering Science and Technology Vol. 2 ,(12), 7045-7054

Farage, M.A., Miller, K.W., Elsner, P., Maibach, H.I. (2008). Intrinsic and extrinsic factors in skin ageing: a review. Int. J. Cosmet. Sci. 30, 87–95.

Guan-qun Chen , Li Ren , Jie Zhang, Barbara M. Reed, Di Zhang, Xiao-hui Shen. (2015). Cryopreservation affects ROS-induced oxidative stress and antioxidant response in Arabidopsis seedlings. Cryobiology , 70, 38–47.

Hyemin Kim, Seyeon Bae, Yejin Kim, Chung-Hyun Cho, SungJoon Kim, Yong-Jin Kim, Seung-Pyo Lee, Hang-Rae Kim, Young-il Hwang, JaeSeung Kang, WangJae Lee. (2013). Vitamin C prevents stress-induced damage on the heart caused by the death of cardiomyocytes, through down-regulation of the excessive production of catecholamine, TNF-α, and ROS productionin Gulo (_/_)$^{\text{Vit C-Insufficient}}$ mice. Free Radical Biology and Medicine. 65. 573–583.

Li Y, Wang B, Wu N, Lan CQ. (2008). Effects of nitrogen sources on cell growth and lipid production of Neochloris oleoabundans. Applied Microbiology and Biotechnology,81(4), 629–36.

Li Y, Horsman M, Wu N, Lan CQ, Dubois-Calero N. (2008). Biofuels from microalgae.Biotechnology Progress. 24(4), 815–20.

Landau, M. (2007). Exogenous factors in skin aging. Curr. Prob. Dermatol. 35, 1–13.

Maya Iv. Mitova, Anatolii I. Usov, Maria I. Bilan, Kamen L. Stefanov, Stefka D. Dimitrova-Konaklieva. Danail P. Tonov, Simeon S. Popov. (1999). Sterols and Polysaccharides in Freshwater Algae Spirogyra and Mougeotia. Z. Naturforsch. 54 ,1016-1020.

Mayalen Zubia , Daniel Robledo , Yolanda Freile-Pelegrin. (2007). Antioxidant activities in tropical marine macroalgae from the Yucatan Peninsula, Mexico J Appl Phycol 19, 449–458

Merichel Plaza, Alejandro Cifuentes and Elena Ibanez. (2008). In the search of new functional food ingredients from algae, Trends in Food Science & Technology. 19. 31-39

Mingjing Gao, ZhenZhao, Pengyu Lv, YuFang Li, Juntao Gao, Michael Zhangd, Baolu Zhao. (2015). Quantitative combination of natural anti-oxidants prevents metabolic syndrome by reducing oxidative stress. Redox Biology. 6, 206–217

Moirangthem Kameshwor Singh, Jai Gopal Sharma, Rina Chakrabarti. (2015). Simulation study of natural UV-B radiation on Catla catla and its impact on

physiology, oxidative stress, Hsp 70 and DNA fragmentation.Journal of Photochemistry and Photobiology B: Biology. 149, 156–163

Meiling Liu, Xinrong Li, Yubing Liu, Yulan Shi , XiaofeiMa. (2015). Analysis of differentially expressed genes under UV-B radiation in the desert plant Reaumuria soongorica. Gene.36, 153-159.

Masaki, H. (2010). Role of antioxidants in the skin: anti-aging effects. J. Dermatol. Sci.58, 85–90.

Mahinda Senevirathne, You-Jin Jeon, Jin-Hwan Ha, Soo-Hyun Kim. (2009). Effective drying of citrus by-product by high speed drying: A novel drying technique and their antioxidant activity. Journal of Food Engineering. 92,157–163.

Nassima Chaher, Stéphanie Krisa. Jean-Claude Delaunay, Stéphane Bernillon, Eric Pedrot, Jean-Michel Mérillon, Djebbar Atmani, Tristan Richard. (2016). Unusual compounds from Galium mollugo and their inhibitoryactivities against ROS generation in human fibroblasts. Journal of Pharmaceutical and Biomedical Analysis. 117,79–84

Nanjo, F., Goto, K., Seto, R., Suzuki, H., Sakai, M., Hara, Y.. (1996). Scavenging effects of tea catechins and their derivatives on 1,1-diphenyl-2-picrylhydrazyl radical.Free radical Biology and Medicine 21, 885–902

Ji-Hyeok Lee , Jong Won Han , Ju-Young Ko et al. (2015). Protective effect of a freshwater alga, *Spirogyra* sp., against lipid peroxidation in vivo zebrafish and purification of antioxidative compounds using preparative centrifugal partition chromatography. J Spring. Appl Phycol. 21, 115–121.

Nalae Kang, Ji-Hyeok Lee, WonWoo Lee et al. (2015). Gallic acid isolated from *Spirogyra* sp. improve cardiovascular disease through a vasorelaxantand antihypertensive effect. Environmental Toxicology and Pharmacology. 39, 764–772.

Kasidit Rattanawong, Kittikhun Kerdsomboon, Choowong Auesukaree. (2015). Cu/Zn-superoxide dismutase and glutathione are involved in response to oxidative stress induced by protein denaturing effect of alachlor in Saccharomyces cerevisiae. Free Radical Biology and Medicine. 89, 963–971

Pinnell, S.R. (2003). .Cutaneous photodamage, oxidative stress, and topical antioxidant protection. J. Am. Acad. Dermatol. 48, 1–22.

Rameshprabu Ramaraj, Yuwalee Unpaprom, Niwooti Whangchai, Natthawud Dussadee. (2015). Culture of Macroalgae Spirogyra ellipsospora for Long-Term Experiments, Stock Maintenance and Biogas Production. Emer Life Sci Res. 1(1), 38-45

Rosen,G.M., Rauckman, E.J. (1980). Spin trapping of the primary radical involved in the activation of the carcinogen N-hydroxy-2-acetylaminofluorene by cumene hydroperoxide hematin. Molecular Pharmacology .17, 233–238

Sheehan J, Dunahay T, Benemann J, Roessler P. (1998). A look back at the U.S. Department of Energy's aquatic species program: biodiesel from algae. NREL/TP-580-24190, National Renewable Energy Laboratory, USA.

S.S. Gill, N. Tuteja. (2010). Reactive oxygen species and antioxidant machinery in abiotic stress tolerance in crop plants, Plant Physiol. Biochem. 48, 909– 930.

Song-Zhi Kong , Hai-Ming Chen, Xiu-Ting Yu, Xie Zhang, Xue-Xuan Feng, Xin-Huang Kang, Wen-Jie Li, NaHuang, Hui Luo, Zi-Ren Su. (2015). The protective effect of 18β-Glycyrrhetinic acid against UV irradiation induced photoaging in mice. Experimental Gerontology. 61,147–155.

Sushil Raut, Santosh Singh Bhadoriya, Vaibhav Uplanchiwara, Vijay Mishrab, Avinash Gahanea, Sunil Kumar Jain. (2012). Lecithin organogel: A unique micellar system for the delivery of bioactive agents in the treatment of skin aging. Acta Pharmaceutica Sinica B (1), 28–15.

Sung-Myung Kang, Areum-Daseul Kim, Soo-Jin Heo, Kil-Nam Kim, Seung-Hong Lee, Seok-Chun Ko, You-Jin Jeon. (2012). Induction of apoptosis by diphlrethorehydroxycarmalol isolated from brown alga, *Ishige okamurae*. Journal of Functional Foods, 4, 433 –439.

Seok-Chun Ko, Seon-Heui Cha & Soo-Jin Heo ,Seung-Hong Lee, Sung-Myung Kang , You-Jin Jeon. (2011). Protective effect of Ecklonia cava on UVB-induced oxidative stress: in vitro and in vivo zebrafish model. J Appl Phycol, 23, 697–708.

VALERIE J. PAUL, MARK M. LITTLER, DIANE S. LITTLER, and WILLIAM FENICAL. (1987). EVIDENCE FOR CHEMICAL DEFENSE IN TROPICAL GREEN ALGA Caulerpa ashmeadii (CAULERPACEAE:CHLOROPHYTA): Isolation of New Bioactive Sesquiterpenoids. Journal of Chemical Ecology, 1171-1185.

V.K. Gupta and A. Rastogi. (2008). Biosorption of lead from aqueous solutions by green algae *Spirogyra* species: Kinetics and equilibrium studies. Journal of Hazardous Materials 152, 407–414.

V.K. Gupta, A. Rastogi, V.K. Saini, N. Jain. (2006). Biosorption of Cu(II) from aqueous solutions by *Spirogyra* species, J. Colloid Interface Sci. 296, 59–63.

V.K. Gupta, A.K. Shrivastava, N. Jain. (2001). Biosorption of chromium(VI) from aqueous solutions by green algae *Spirogyra* species, Water Res. 35 (17), 4079–4085.

N.R. Bishnoi, M. Bajaj, K. Sanatomba. (2005). Biosorption of zinc(II) using *Spirogyra* species from electroplating effluent, J. Environ. Biol. 26 (4), 661–664.

S. Venkatamohan, S.V. Ramanaiah, B. Rajkumar, P.N. Sharma. (2007), Removal of fluoride from aqueous phase by biosorption onto algal biosorbent *Spirogyra* sp. I02: sorption mechanism elucidation, J. Hazard. Mater. 141, 465–474.

Zhongshan Zhanga,b, Feng Wangc, Xiaomei Wanga, Xiaolei Liud, Yun Houb, Quanbin Zhang. (2010). Extraction of the polysaccharides from five algae and their potential antioxidant activity in vitro. Carbohydrate Polymers . 82. 118–121.

Acknowledgement

I would like to offer my first and foremost thanks to my supervisor, professor You-Jin Jeon, department of Marine Life Science, Jeju National University, Jeju, Korea. His kindly guidance, help, understanding and most importantly his high academic level and wonderful life experience, encouraged me to keep moving forward. During my master course period in Jeju National University, I have adored my supervisor as a great advisor. It is really my great honor as a strudent to be supervised by him.

I would like to thank my parents, family members and all of my relatives for their love, care and support. I want thanks my parents for their effort to take good care of me since birth. They at their best tried to give me all the finest things that they can afford, for my well being.

I would like to extend my thank and gratitude to Dr. Yong Li, Changchun University of Chinese Medicine, Changchun, China for recommendeding me to work under Prof. You-Jin Jeon. He was also a student of Prof. You-Jin Jeon and he was my superviser when I was studing in China.

Also I would like to thank Prof. Jiyu Gong, Prof. Zhihong Wang, Prof. Peng Yu, Dr. Ye Wang, Dr. Na Li, Changchun University of Chinese Medicine, Changchun, China, and Prof. Guirong Zhang, Jilin University, Changchun, China. Thanks for their help, believe and the academic guidance.

Especially, I would like to thank my colleagues Dr. Won-Woo Lee, Dr. Ji-Heyok Lee, Dr. Ju Young Ku, Eun-A Kim, Jea Young Oh, Nalse Kang, Shanura Fernando, Seo Young Kim, Hyun Soo Kim, H.H. Chaminda Lakmal, Wen Jian , Asanka Sanjeewa,

Nehal Osman, Yoon Teak Kim, Hye-Won Yang and Hyoung Ho Kim, for their kind help for my research work and my daily life in Korea.

Last but not least, I would like to express my grateful appreciation to my Chinese friends which got to known each other in Korea. Namely Sheng Piao, Zhen Liu, Hao Yu, Ya Zhang, Lei Song, Yuling Ding, Zhenyu Zhong, Ye Tian, Xiateng Hu, Wenhao Shi, Sujuan Jin, Shuo He, Zhangming Helian and others. Thank you guys for accompanying me and for the unforgettable times and memories in this foreign land.

Thank you

Lei Wang

Jeju National University,

Republic of Korea.

February, 2016.